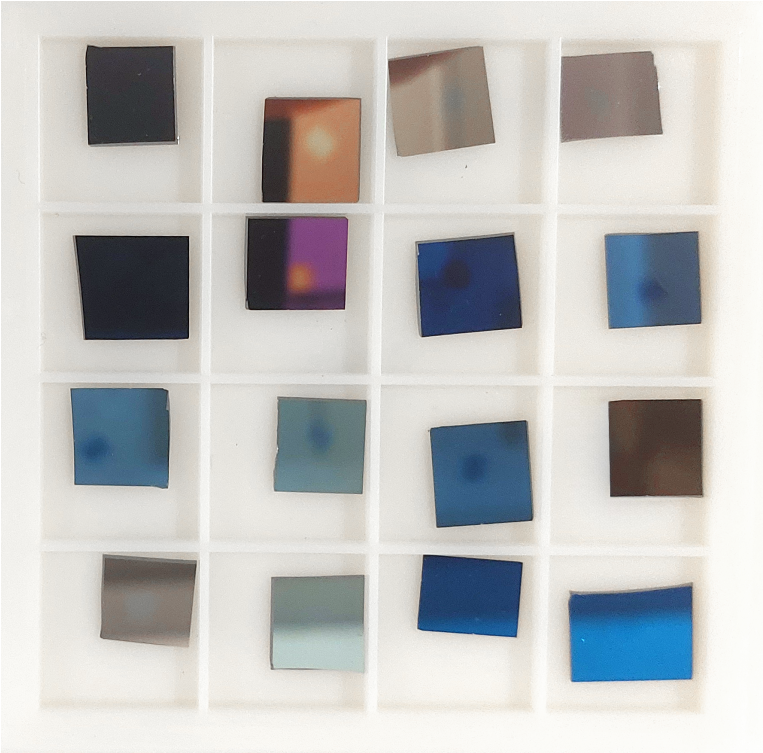

Optimisation of Plasma Enhanced Chemical Vapour Deposition for Silicon Nitride Photonics using Optimal Design of Experiments

Erasmus Mundus Master in Nanoscience and Nanotechnology
Specialisation track: Nanophysics

Local Promoter: Prof. Dr. Victor Torres-Company
KU Leuven Co-Promoter: Prof. Dr. Pol Van Dorpe

MIA BUCHMAYR

DEPARTMENT OF MICROTECHNOLOGY AND NANOSCIENCE
CHALMERS UNIVERSITY OF TECHNOLOGY
Gothenburg, Sweden 2025
www.chalmers.se

Master's thesis 2025

Optimisation of Plasma Enhanced Chemical Vapour Deposition for Silicon Nitride Photonics using Optimal Design of Experiments

MIA BUCHMAYR

CHALMERS
UNIVERSITY OF TECHNOLOGY

Department of Microtechnology and Nanoscience
Division of Photonics
Integrated Ultrafast Photonics Group
Chalmers University of Technology
Gothenburg, Sweden 2025

Optimisation of Plasma Enhanced Chemical Vapour Deposition for Silicon Nitride Photonics using Optimal Design of Experiments

MIA BUCHMAYR

Local Promoter: Victor Torres-Company, Chalmers University of Technology
Co-Promoter: Pol Van Dorpe, KU Leuven & imec
Daily Supervisor: Vijay Shekhawat, Chalmers University of Technology

Master's Thesis 2025
Department of Microtechnology and Nanoscience
Division of Photonics
Integrated Ultrafast Photonics Group
Chalmers University of Technology
SE-412 96 Gothenburg
Telephone +46 31 772 1000

Typeset in LaTeX
Printed by Chalmers Reproservice
Gothenburg, Sweden 2025

MIA BUCHMAYR
Department of Microtechnology and Nanoscience
Chalmers University of Technology

Abstract

There have been many advances in silicon nitride based integrated photonics, enabling a variety of interesting applications. The deposition of high quality and low loss silicon nitride (SiN) during the fabrication of waveguides is essential for creating useful devices. Low temperature alternatives to low pressure chemical vapour deposition (LPCVD) such as plasma enhanced chemical vapour deposition (PECVD) are required to enable back-end-of-line (BEOL) integration.
The difficulty with optimising PECVD deposition of silicon nitride is that it includes many process parameters that affect the deposition and resulting properties of the film. Thus, optimisation of the PECVD recipe requires a strategic approach to the experimental design.
In this work, a technique called optimal design of experiments (DoE) is used to obtain an overview of the PECVD factor's influence on silicon nitride properties, and to predict the optimal PECVD recipe. With the help of the statistical software JMP the optimal DoE for PECVD deposition of SiN created, significant factors and correlations identified, and optimal PECVD factor combinations predicted. Ellipsometry measurements provide data regarding the responses of interest, namely thickness uniformity, refractive index, and extinction coefficient of the SiN film.
It is found that the refractive index is correlated with the ammonia gas flow rate and the extinction coefficient. Most PECVD factors appear to be relevant, in particular the ammonia gas flow rate for the refractive index and the extinction coefficient, and the frequency mode for the thickness uniformity. In addition, two-factor interaction effects are present in the PECVD process and affect the relationship between process parameters and responses. Furthermore, in terms of stoichiometry, silicon nitride films with a refractive index close to two are found to be silicon rich. The testing of predicted recipes shows that the three responses, i.e. refractive index, extinction coefficient and thickness uniformity, cannot be optimised simultaneously to the desired outcome. However, when considering a stoichiometric Si/N ratio instead of the refractive index, predicted recipes result in improved and equally good responses compared to default PECVD and LPCVD recipes, respectively.
This approach of optimal DoE shows promising potential and could be interesting to explore further, especially regarding the optimisation of other relevant fabrication steps affecting the propagation losses in waveguides.

Keywords: Silicon Nitride, PECVD, Photonic Integrated Circuits, Optimal Design of Experiments.

List of Acronyms

Acronyms used in this thesis are listed in alphabetical order below:

CMOS	Complementary Metal-Oxide-Semiconductor
DoE	Design of Experiments
ECR-PECVD	Electron Cyclotron Resonance Plasma-Enhanced Chemical Vapour Deposition
HF	High Frequency
ICPCVD	Inductively Coupled Plasma Chemical Vapour Deposition
JMP	JMP Statistical Discovery Software
LF	Low Frequency
LPCVD	Low Pressure Chemical Vapour Deposition
MSE	Mean Squared Error
MF	Mixed Frequency
N-rich	Nitrogen-rich
PECVD	Plasma Enhanced Chemical Vapour Deposition
PICs	Photonic Integrated Circuits
RF	Radio Frequency
sccm	Standard Cubic Centimetres per Minute
SC-1	Standard Clean 1
SC-2	Standard Clean 2
SiN	Silicon Nitride
Si/N	Silicon to Nitrogen Ratio
Si-rich	Silicon-rich
XPS	X-ray Photoelectron Spectroscopy

Contents

List of Figures

List of Tables

1
Introduction

Photonic technologies are very powerful, enabling many useful advances and application in the fields of data transmission, precise sensing, and high resolution imaging. This has led to advances in both applications and fundamental research [1]. Traditionally, this involves huge setups on optical tables with hundreds of discrete optical components, such as lenses, mirrors, beam splitters, and lasers. This results in a highly complicated, costly and sensitive setups, for which a lot of space, time and work has to be dedicated. Integrated photonics addresses this problem, by enabling the creation of equivalent functionalities on chip, allowing a more scalable and efficient solution [1]. Waveguides and other components can be fabricated as integrated structures onto the surface of a substrate creating integrated photonics circuits. These integrated photonic circuits can transmit and process light on a chip, similar to how electronic signals are processed in integrated electronic circuits on chip. As a result, the size of the optical system can be dramatically miniaturised, allowing compact and robust high density integration of components on chips in the form of photonic integrated circuits (PICs). The use of mature semiconductor manufacturing processes for the fabrication of PICs facilitates scalability, and allows production of higher volumes at lower cost, making it more economically efficient [2].

One of the most mature material platforms for integrated photonics is silicon. It has a long history in semiconductor industry and has become an important material for photonics in the last few decades. More importantly, silicon is complementary metal-oxide-semiconductor (CMOS) compatible, allowing for seamless integration with existing processes and thus, making it scalable and cost-effective [1]. Silicon has a high refractive index around 3.5–3.9, resulting in very high refractive index contrast between the silicon core and silica (SiO_2) cladding of a waveguide, which allows the design of small structures [1, 3]. The transparency window of silicon, i.e. the wavelength range in which there are low absorption losses, is from 1.1–3.7 µm, propagation losses of 1–2 dB/cm are typical, and active photonic devices such as modulators are supported [1]. However, there are some drawbacks to the silicon platform: the rather high thermo-optic coefficient, which can lead to temperature dependent changes in the refractive index; the issue with two-photon absorption rendering the huge Kerr-nonlinearity useless in the near-infrared and visible wavelength ranges; the lack of ultra-low propagation losses; and the inability to operate in the visible range of light [3]. These can be overcome by using silicon nitride (SiN) instead. Silicon nitride can achieve lower propagation losses (0.01 dB/cm), has a wider transparency window down to the visible range (400 nm – 6.7 µm), a lower thermo-optic coefficient leading to improved thermal stability, and is better suited for non-

linear operations because, although it has a weaker Kerr non-linearity, two-photon absorption is not a concern [3–6]. In addition, silicon nitride has a moderately high refractive index contrast and is CMOS compatible as well.
Over the last three decades there has been a lot of improvement in silicon nitride photonics. Applications like ultra-low linewidth lasers, optical frequency combs, optical modulators, tunable lasers and filters have been developed [2, 5, 7]. Silicon nitride photonics are of interest in various different fields: from quantum computing, high-performance computing, and telecom applications, to sensing applications like LiDAR, spectroscopy, as well as in atomic physics and life sciences [5, 8]. The prospect of using silicon nitride combined with hybrid or heterogenous integration techniques enables even more exciting and complex applications and prospects [8].
A very common method for depositing silicon nitride films during the fabrication of components like waveguides is Low Pressure Chemical Vapour Deposition (LPCVD). LPCVD is a chemical vapour deposition technique using low chamber pressure and high temperatures (700–900°C) to form reactive gaseous species, which react at the substrate surface to form the silicon nitride layer [9]. Typically, during the fabrication of silicon nitride waveguides, an annealing step is performed at temperatures up to 1200°C after the SiN deposition to remove any hydrogen incorporated in the SiN layer, since hydrogen bonds, especially N-H bonds, can act as absorption centres at the wavelength of interest (1550 nm), leading to high absorption losses [10, 11]. This way ultralow-loss SiN waveguides with propagation losses of lower than 0.01 dB/cm can be fabricated via LPCVD [4].
However, these high temperature processes can pose a problem, especially when the goal is to combine conventional CMOS technology and integrated photonic circuits on the same chip. This is because the proper functionality of CMOS electronics is highly dependent on precise doping levels. Doping in turn, is highly temperature sensitive. Already small changes in temperature can cause unwanted doping diffusion modifying doping profiles, and thus, resulting in dysfunctional devices [12]. Additionally, high processing temperatures are problematic for enabling back-end-of-line integration (BEOL) and can be hindering when wanting to combine different materials, where some might have lower melting temperatures [13]. Therefore, alternative, low-temperature processes for silicon nitride deposition have been investigated. For example, Plasma Enhanced Chemical Vapour Deposition (PECVD) or sputtering [14]. PECVD is a chemical vapour deposition technique similar to LPCVD, but uses a highly energetic plasma environment instead of high process temperatures to create reactive gaseous species, which later form the silicon nitride layer [15]. The problem with these alternative deposition techniques is, that they typically result in higher losses than LPCVD by multiple orders of magnitude [16]. Therefore, the optimisation of low-temperature SiN deposition processes to reduce waveguide losses remains a relevant and active research topic.

1.1 Research Question

Given the importance of developing low-temperature deposition processes for the fabrication of low-loss silicon nitride layers, this thesis focuses on improving PECVD deposited silicon nitride for integrated photonics. The difficulty with optimising the

PECVD process is the multitude of different process parameters that can affect silicon nitride deposition and the resulting film properties. PECVD process parameters that have been investigated in the literature include: the gaseous precursors used, the total gas flow rate, the relative ratio of gas flow rates from different gas species to each other, the pressure, the RF power, frequency of the oscillating electric field, plasma density, or even mechanical engineering considerations such as the distance between electrodes [17, 18]. In addition, there may be interaction effects between two or more factors, meaning that one factor can affect how another factor influences the deposition process or film properties. This further complicates drawing universally valid conclusions about the relationships between process parameters and outcomes.
Furthermore, the more factors are to be investigated, the larger the experiment has to be in order to determine the relevant factors and trends. Even if only six PECVD factors are investigated, approaching this problem by simply trying out all the possible combinations is impossible. For instance, investigating six of these factors, e.g. pressure, power, temperature, and gas flow rates of three involved gases, at ten different parameter settings each, would already result in a million different possible combinations of PECVD factors. In the case of only testing three settings for each of the six factors, this still results in 729 different PECVD recipes. This highlights the need for a more strategic, systematic experimental approach such as Design of Experiments (DoE). Design of Experiments involves the use of powerful statistical methods to plan and analyse experiments in a way that allows effective and efficient investigation of experiments containing multiple factors. It is used to increase process performance, improve yield, robustness, or reduce variability [19]. Hence, DoE techniques can be used to arrive at a feasible experimental design plan.
In this thesis, the goal is to investigate and tune the PECVD recipe for silicon nitride deposition in the context of integrated photonics. In particular, the optimal combination of PECVD factor settings is to be found. In the course of this, relevant PECVD factors are to be identified with regard to their effect on the refractive index, extinction coefficient, and thickness uniformity of the deposited silicon nitride film. To achieve this task, an optimal design of experiment is designed to investigate the six PECVD factors: pressure, RF power, frequency mode, and gas flow rates of silane, ammonia and nitrogen. The responses of interest corresponding to the experimental design runs are measured using spectroscopic ellipsometry. From this, optimal PECVD recipes are predicted and their performance tested to arrive at an improved PECVD recipe.
In the following chapters, first, some background information on the PECVD process, the state of the art PECVD-deposited silicon nitride, and measurement methods used is given. Then, the exact methodology used to design the optimal experiment and predict the optimal PECVD recipes, as well as the process flow followed for the deposition and subsequent measurements of silicon nitride films is described. This is followed by a presentation and discussion of the obtained results. Finally, the conclusions drawn from this investigation are stated and suggestions for future continuation of this work are made.

2
Background Information

This chapter provides some background information on the material silicon nitride and its optical properties, the process of plasma enhanced chemical vapour deposition and how the different settings can affect the properties of SiN films. Additionally, an explanation is given for the optimal design of experiments, as well as the working principle of the measurement tools used.

2.1 Silicon Nitride Photonics

Silicon nitride is a dielectric material that is popular in photonics and semiconductor technology [6]. It is typically amorphous, when grown by chemical vapour deposition techniques, although the growth of crystalline SiN films is being investigated [20]. Silicon nitride has a large bandgap of approximately 5.3 eV making it a good insulator and resulting in a wide transparency window. Especially, stoichiometric silicon nitride (Si_3N_4) is said to have many benefits [21]. For instance, ultralow propagation losses (< 0.01 dB/cm), lack of two-photon absorption at telecommunication wavelengths, a broad optical transparency window from the visible to the infrared region (400 nm – 6.7 µm), and the capability to handle high powers [3, 21]. In integrated photonics, the waveguide core can be made from silicon nitride. During the fabrication step of a waveguide, a silicon nitride film is deposited on top of cladding material like silica, then patterned and etched to obtain the intended waveguide geometry. The idea is to achieve integrated waveguides that can confine and guide light with minimal propagation losses.
These propagation losses consist of scattering losses, absorption losses, losses due to impurities, and bending losses for curved waveguides [22]. Scattering losses, occurring due to sidewall roughness resulting from the etching process during waveguide fabrication, are said to contribute to the propagation losses the most in highly confined waveguide geometries [13]. However, in the context of this thesis the losses due to intrinsic material absorption and impurities are the relevant type of loss, since these can be influenced by the chosen method of silicon nitride deposition. Intrinsic absorptions arise from fundamental physical processes in the material such as electronic transitions and vibrational modes [22]. In dielectric materials like silicon nitride, electronic transitions can lead to absorption in the ultraviolet, while vibrational modes cause absorption in mid-infrared regions, respectively [4]. The spectral regions of increased absorption can be observed from the imaginary component of the refractive index.
The complex refractive index is wavelength-dependent and describe how light inter-

acts with a given material and can be written as [23–25]:

$$\tilde{n}(\lambda) = n(\lambda) + ik(\lambda) \tag{2.1}$$

where n denotes the real part of the refractive index and k, the imaginary part, is known as extinction coefficient. The refractive index and extinction coefficient are interconnected via the Kramers-Kronig relationship [23]. The refractive index n describes how the phase velocity of light in a material compares to the speed of light in vacuum. The extinction coefficient k is related to the absorption coefficient α and as a result to the loss of light intensity $I(x)$ in the material [26]:

$$\alpha = \frac{4\pi k}{\lambda} \tag{2.2}$$

$$I(x) = I_0 e^{-\alpha x} \tag{2.3}$$

In the context of PICs, a minimal extinction coefficient, as close to zero as possible, is desirable at the wavelength of interest, as this should result in low light absorption in the waveguide material. As for the real part of the refractive index, the desired value can depend on the use case. Often, a value close to two is desired, because this is associated with stoichiometric silicon nitride [27]. A greater refractive index ($n > 2$) indicates a silicon-rich material composition, while nitrogen-rich silicon nitride leads to a smaller refractive index [28]. In general, both the refractive index and extinction coefficient of silicon nitride decrease as the wavelength of light increases due to the decreased photon energy at higher wavelengths. An example of this is shown in Figure 2.1.

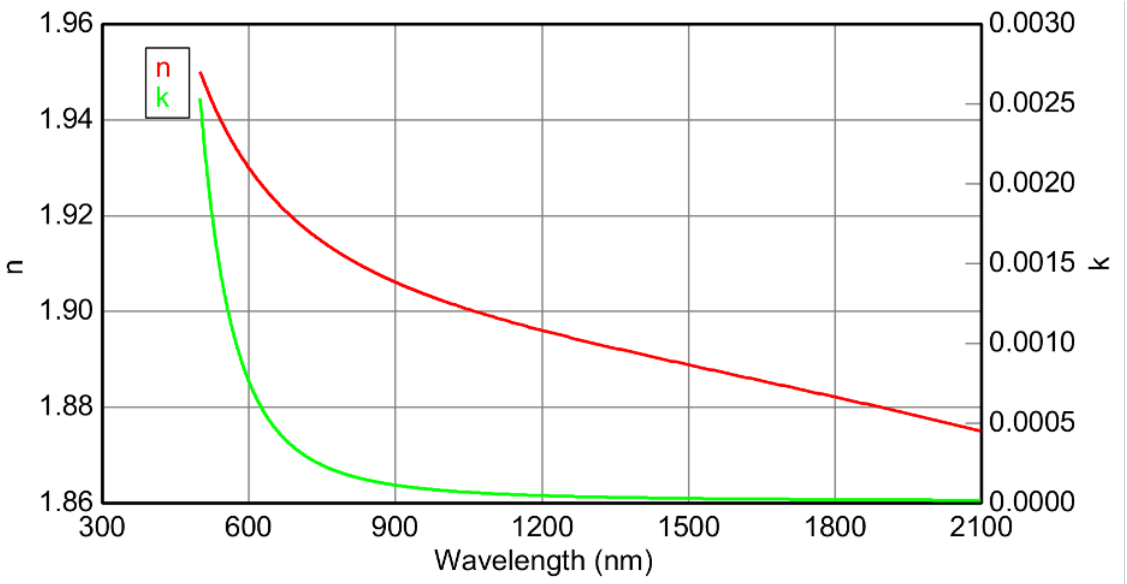

Figure 2.1: Refractive index and extinction coefficient of a silicon nitride film across a range of wavelengths. (Obtained from ellipsometer measurements of the SiN sample fabricated with the default PECVD recipe.)

2.2 Plasma Enhanced Chemical Vapour Deposition

Plasma enhanced chemical vapour deposition (PECVD) is a chemical vapour deposition technique that uses plasma to generate a highly energetic environment for the formation of silicon nitride films. The main benefit of this deposition method is its ability to operate at low process temperatures, typically below 400 °C and even as low as 80 °C, making it suitable for fabricating components and devices sensitive to high temperatures [29, 30].
The deposition of a film via PECVD starts with the introduction of gaseous precursors into a low-pressure chamber. In the case of silicon nitride deposition, typical precursors are silane and ammonia. A radio frequency power source is applied to the electrodes, resulting in an oscillating electric field. For a capacitively coupled PECVD machine, as used in this work, the electrodes take the form of parallel plates, as illustrated in Figure 2.2. The oscillating electric field accelerates free electrons, which then collide with precursor gas molecules, causing chemical bonds to break, and resulting in ions, electrons and excited neutral species, forming the plasma [29]. Once the reactive species have formed, they are driven toward the wafer surface by both diffusion and drift. The electric field gradient contributes to driving the charges species towards the substrate [31]. Upon reaching the substrate surface, the reactive species adsorb and undergo chemical reactions, forming Si-N bonds and thus, gradually building up the silicon nitride film over time.

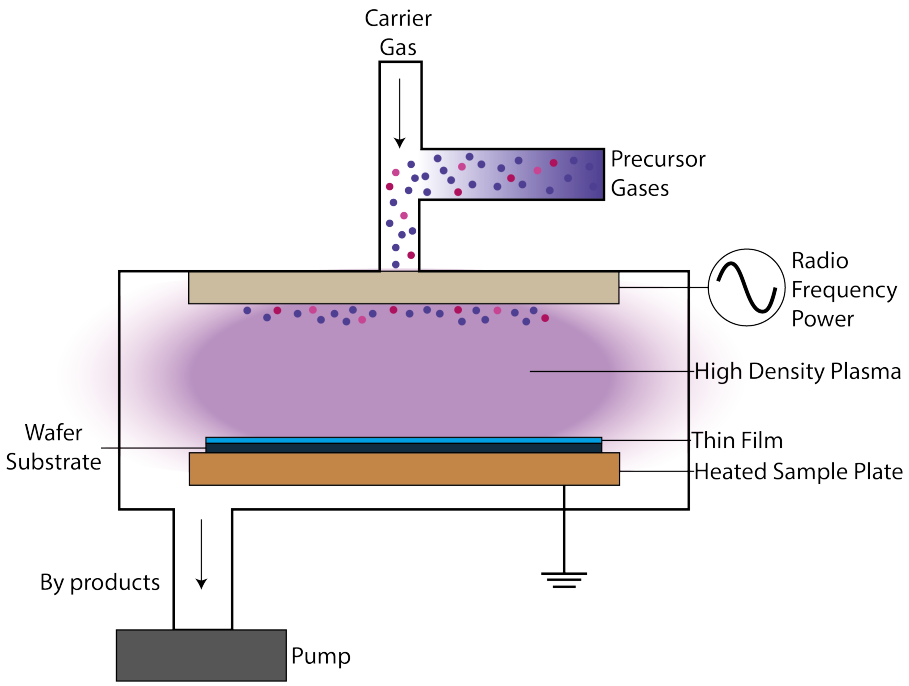

Figure 2.2: Illustration of a plasma enhanced chemical vapour deposition chamber.

Many of the process parameters involved in PECVD can affect the deposition process and the resulting film properties. Typically, the gas flow ratio of precursor gases is a decisive aspect with respect to the composition of the formed material layer [32]. Other parameters such as pressure or temperature are more known to affect the deposition process itself, such as the deposition rate [18]. A more detailed explanation about how PECVD process factors affect silicon nitride films is given below.

2.2.1 Effect of PECVD Process Parameters on Silicon Nitride

The precursor gases used for film deposition in PECVD are a decisive factor for the film's elemental composition. Typically, for the deposition of silicon nitride using PECVD, silane (SiH_4) and ammonia (NH_3) are used as precursors, while nitrogen (N_2) is used as carrier gas. Some of the greatest improvements regarding the reduction of losses in PECVD deposited silicon nitride waveguides have been observed when using a different precursor gas for providing the silicon atoms. The use of deuterated silane (SiD_4) instead of SiH_4 leads to an absence of the Si-H and N-H absorption peaks in the C-band (1530—1565 nm). As a result, waveguide losses at these wavelengths are typically lower than if the precursor SiH_4 is used [21, 33]. The problem with this SiD_4 precursor is that it is not as commonly available in cleanrooms as SiH_4 is. This is the case for this thesis work, which is why deuterated silane precursor is not used despite its advantages. Furthermore, NH_3-free PECVD recipes, where the nitrogen is obtained from the dissociation of N_2 instead, have been reported to be beneficial for reducing the hydrogen content and therefore, for reducing optical absorption and losses in silicon nitride films [6, 13, 15].
The gas flow rate ratio of ammonia and silane have been widely reported to affect film properties such as refractive index, defect states and bandgap. An increased silane gas flow rate leads to an increased silicon content in the film because more Si-Si bonds form and thus, a greater refractive index [15, 30, 34]. On the other hand an increase in ammonia leads to a decreased refractive index and increased optical bandgaps [34, 35]. The reason for this is that more Si-N and less Si-Si bonds are formed at increased ammonia gas flow, resulting in a decreased Si/N ratio and subsequently a reduced refractive index because nitrogen has a lower refractive index than silicon [35, 36]. Furthermore, increasing ammonia flow rate has been found to be related to a decrease in defect states in SiN films, influencing light trapping at these defect sites and thus, transmittance [35]. As for the nitrogen gas flow rate, it is not normally considered as a reaction gas, with the exception of NH_3-free recipes, but rather explored with respect to its influence on deposition rate. Nevertheless, an increase in nitrogen gas flow rate favours an increase in the nitrogen content of the SiN film, and therefore, may result in a decreased refractive index [15]. Mostly, the ratio of different precursor gases is considered as the determining factor for the resulting silicon-to-nitrogen ratio in the deposited film and thus, also for the refractive index and film density [30].
The influence of the frequency mode in PECVD is mostly mentioned in the context of SiN film stress. Low frequency mode leads to compressive stress, high frequency

mode to tensile stress, and the mixed frequency mode to low stress films [16]. In terms of refractive index low frequency mode seems to result in the lowest refractive index values, while mixed frequency mode gives the highest refractive index [16]. Moreover, it has been mentioned in literature that varying frequency of the RF power in PECVD affects the optical losses via the breakage of hydrogen bonds [21].

Deposition temperature can influence the refractive index and also the mass density of the deposited silicon nitride film. The amount of hydrogen bonds present in the film is temperature dependent. Lower deposition temperatures result in lower mass density and refractive index of SiN films [37]. For similar reasons, post-deposition annealing temperature, if an annealing step is performed, is also a decisive factor on the proprieties of silicon nitride, whereby higher annealing temperatures can result in an increased density and refractive index [37].

Pressure has been reported to influence the refractive index and thickness uniformity. An increase in pressure apparently leads to an increase in refractive index due to better gas distribution and higher plasma density [15, 30]. However, other findings report an opposite relation, where increasing pressure in PECVD increases the non-uniformity or decreases the refractive index [18, 30, 34]. It seems that it is relevant whether high or low pressure ranges are investigated.

As for how the RF power affects silicon nitride in PECVD, one report states that an increase in power is disfavourable for both the uniformity and achieving a higher refractive index [15]. Another study finds that increasing RF power provides more energy and therefore increases the plasma density and reactive content [30].

2.3 Optimal Design of Experiments

Optimal Design of Experiments is a statistical approach to strategically plan experiments in order to maximise the information gained from the experiment, while minimising the number of experimental runs and thus, minimising the cost and effort [38]. In an optimal DoE the most informative combinations of input variables are selected to study their effect on the output being investigated. Unlike traditional DoE approaches, such as full factorial or central composite designs, in optimal DoE one is not constrained to rigid designs [39]. Instead the optimal DoE approach allows the tailoring of the experimental design to the real-world situation at hand. For example, in case of hard-to-change factor settings, or factor combinations being unfeasible in the actual experimental process, this can be accounted for in optimal DoE.

At the start of designing an experiment, a linear regression model, which describes the process and includes the effects that are presumed to be of interest, is defined. When investigating the relevant factors in a process, such a model typically includes first-order terms representing the main effects (linear effects) of the process factors. It can also include second-order effects such two-factor interaction effects, or quadratic effects. Two-factor interaction effects are present, when the impact of one process factor depends on the setting of another process factor [38]. Quadratic effects describe curvature present in the relationship between process factors and the process response being investigated. The regression model for a complete quadratic

model would be [38]:

$$Y = \beta_0 + \sum_{i=1}^{k} \beta_i x_i + \sum_{i=1}^{k-1} \sum_{j=i+1}^{k} \beta_{ij} x_i x_j + \sum_{i=1}^{k} \beta_{ii} x_i^2 + \varepsilon \tag{2.4}$$

where Y is the observed response, x_k the experimental factors, β_k the model coefficients, and ε the random error. This regression model can be written in matrix form as follows [38]:

$$\boldsymbol{Y} = \boldsymbol{X}\boldsymbol{\beta} + \boldsymbol{\varepsilon} \tag{2.5}$$

where $\boldsymbol{Y}$ represents the observed responses from n experimental runs, $\boldsymbol{\varepsilon}$ is a vector denoting the random error, $\boldsymbol{\beta}$ is vector containing the $k+1$ regression coefficients, k is the number of process factors being investigated, and $\boldsymbol{X}$ is the model matrix of size $n \times (k+1)$ encoding the effects of the process factors and the intercept. The regression model is fit to the experimental data using ordinary least squares estimation. The estimator for the unknown model coefficients is thus [38]:

$$\hat{\boldsymbol{\beta}} = (\boldsymbol{X}^{\boldsymbol{T}}\boldsymbol{X})^{-1}\boldsymbol{X}^{\boldsymbol{T}}\boldsymbol{Y} \tag{2.6}$$

whereby $(\boldsymbol{X}^{\boldsymbol{T}}\boldsymbol{X})^{-1}$ corresponds to the variance of the coefficient's estimates, determining the precision of estimated effects. It is also used for the calculation of the information matrix. The information matrix contains the available information about the model's parameters and is important for the experimental design generation. The information matrix is written as [38]:

$$\boldsymbol{M} = \frac{1}{\sigma_\varepsilon^2}\boldsymbol{X}^{\boldsymbol{T}}\boldsymbol{X} \tag{2.7}$$

The optimal experimental design is generated via the coordinate-Exchange algorithm [40]. The so-called coordinate points show the different factor settings of different experimental runs within the design space. For example, one coordinate point represents one of the experimental runs. The coordinates of that point indicate the level setting of the investigated process factors. The coordinate algorithm walks through the design one coordinate at a time, i.e. it changes one process factor level in one algorithm iteration, in an attempt to find an improvement in the design's quality [38]. The design quality is typically measured by a numeric optimality-criterion, which is derived from the information matrix. A common optimality criterion is to maximise the determinant of the information matrix, which is called the D-optimality criterion. Other optimality criteria are the the I-optimality criterion, which minimises the average prediction variance across the design space, or the G-optimality criterion, which is used to find designs that minimise the maximum prediction variance across the experimental region [38, 40].
Figure 2.3 illustrates the working principle of the coordinate-exchange algorithm. The Coordinate-Exchange algorithm starts off with a random design, meaning that for each experimental run, random settings are assigned to each of the process factors being investigated. The algorithm then proceeds to visit one coordinate at a time (one factor level in each iteration). It begins with the first factor in the first experimental run. The algorithm tests alternative levels, the two most

extreme values for that factor [40]. Then the information matrix and the optimality criterion are computed. If this results in an increased optimality criterion, meaning the overall design has improved, the coordinate value in the table is replaced by this alternative value. This process is then repeated for the second factor of the first run. This iterative procedure repeats through all experimental runs multiple times until no change in any coordinate improves the design further [38, 40]. At this point the optimal experimental design, or at least the one that best satisfies the selected optimality criterion, has been created.

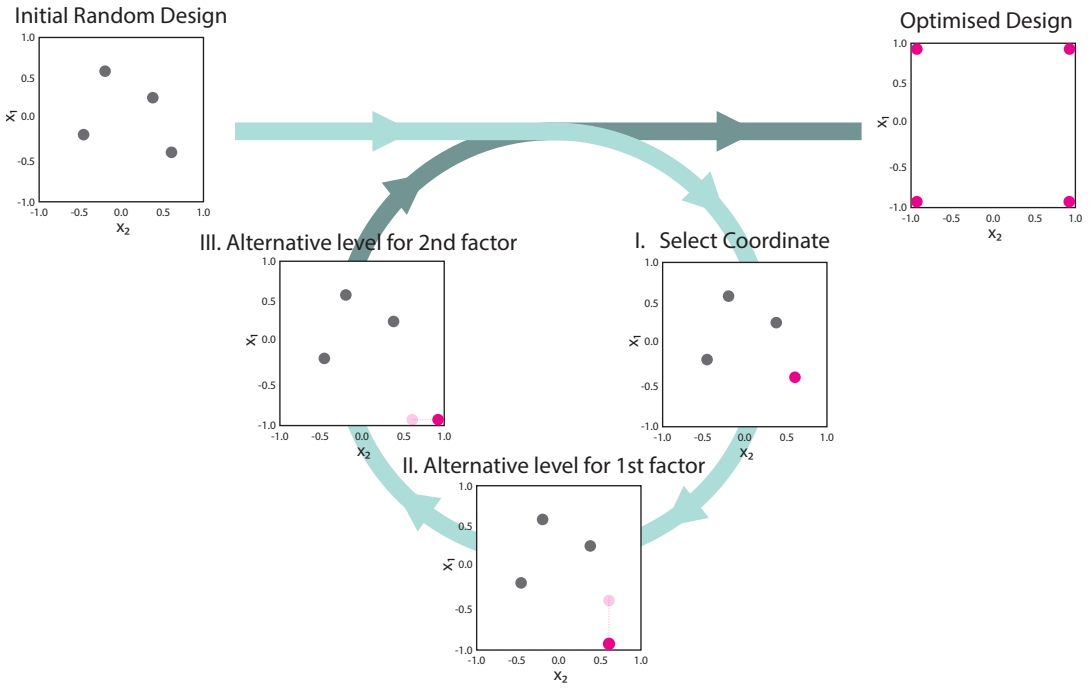

Figure 2.3: Illustration of the coordinate-exchange algorithm used to arrive at the optimal experimental design.

2.4 Measurement Tools

In this section the tools used to perform the measurements of the deposited silicon nitride film are described.

2.4.1 Ellipsometry

Ellipsometry is a non-destructive optical technique used to determine the thickness and optical properties of thin films and bulk materials. It is a widely used method for semiconductor and dielectric films, due to its high sensitivity and accuracy in determining film thickness [41]. It is based on analysing changes in the polarisation state of light after it reflects off a sample surface. These changes, measured across a range of wavelengths from ultraviolet to near infrared light, provide detailed information about the sample's thickness, refractive index (n), and extinction coefficient

(k). Spectroscopic ellipsometry is particularly well-suited for characterizing thin films, including those with thicknesses below 10 nm. Due to its high sensitivity to phase changes in light, it can detect variations in thickness down to the sub-angstrom level [26]. The typical accuracy of ellipsometry thickness measurements lies at 0.1–0.2 nm [41]. A wide range of materials can be analysed using ellipsometry, including transparent polymers, dielectric materials, metals, and semiconductors like silicon [41].
The basic setup of an ellipsometry measurement is illustrated in Figure 2.4. A beam of linearly polarised light is directed at the sample at an oblique angle (typically between 65° and 80°). Upon reflection, the light becomes elliptically polarised and is then detected. By comparing the reflected light to the incident light, information about the sample's optical properties is extracted [41].

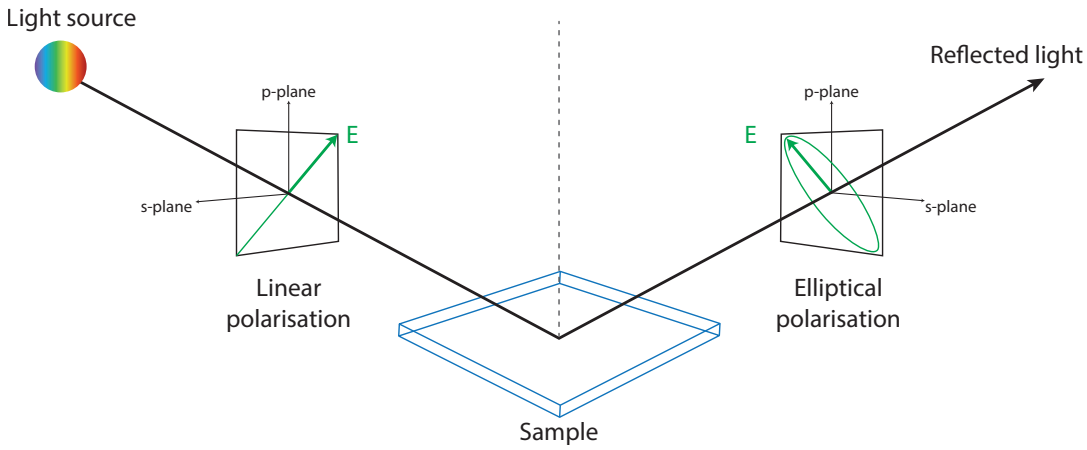

Figure 2.4: Measurement principle of spectrometric ellipsometry based on the change in polarisation of the light reflected from the sample compared to the incident light.

Light is an electromagnetic wave, and its electric field oscillates perpendicular to the direction of propagation. The polarisation state of light, specifically the electric field components parallel (p) and perpendicular (s) to the plane of incidence, is central to ellipsometry measurements [41]. Light can be linearly polarised, in which case the p- and s- components are in phase. If the electric field amplitudes of these two components are equal, but the a phase difference of $\pi/2$ exists, the light in circularly polarised [42]. Elliptical polarisation occurs at arbitrary amplitudes and phase differences.
When light interacts with a sample, its polarisation state changes due to the material's optical properties. These changes are quantified using two parameters: Ψ, the amplitude ratio between p- and s- polarised light, and Δ, the phase difference existing between the two components. These two parameters are obtained at a known wavelength range and incident angle. The complex reflectance ratio encapsulates how the sample modifies the polarisation of the incident light and is defined as [41]:

$$\rho = tan(\Psi)e^{i\Delta} \tag{2.8}$$

The behaviour of Ψ and Δ reveals material characteristic like transparency, absorption, and film thickness of the sample.
To extract physical quantities like the thickness, refractive index and extinction coefficient, a model-fitting procedure is used. This involves choosing a suitable model based on sample structure and material type, whereby a custom model can be built or predefined models for common materials can be used in the ellipsometer software. Additional parameters like surface roughness or interface layers can also be included, if necessary, to improve the accuracy of the model. For an amorphous, dielectric material like silicon nitride, the Tauc-Lorentz oscillator model is commonly used as dispersion model because it effectively captures the material's optical behaviour [43].
The model-fitting process compares the measured Ψ and Δ values to those predicted by the selected model [26]. First, Ψ and Δ are calculated form the model and compared to the experimental data. Then the model parameters (e.g. thickness) are adjusted iteratively until the discrepancy between model and measurement is minimised. The quality of the fit is quantified using the mean squared error (MSE), whereby a lower MSE indicates a better match between the model and the actual sample [26]. Accurate fitting is essential for determining the optical properties of the sample reliably.

2.4.2 X-ray Photoelectron Spectroscopy

X-ray photoelectron spectroscopy (XPS) is a surface measurement technique, that can be used to determine surface composition and the chemical states of the elements present within 10 nm of the surface [44]. This provides detailed information about the material composition. An X-ray is directed at the sample causing core

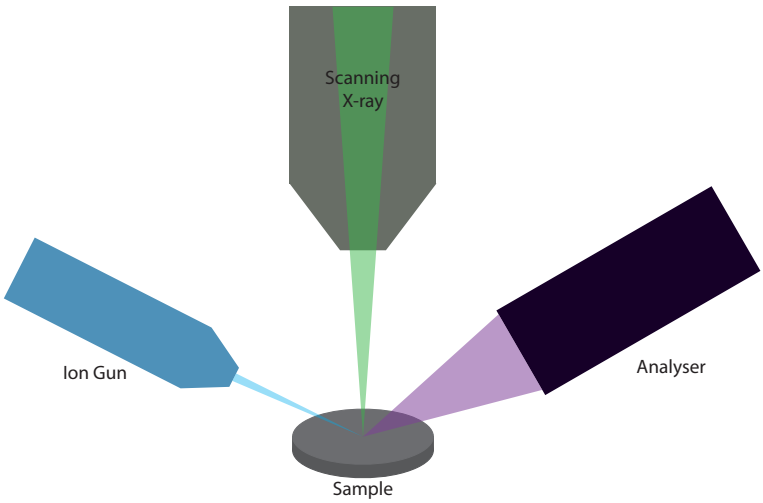

Figure 2.5: Illustration of the XPS probe setup.

electrons to be emitted from the sample surface. These emitted electrons are detected, whereby the kinetic energy of the detected electrons is measured [44]. The

energy of the X-ray is varied, resulting in a XPS spectrum being obtained, which depicts the number of electron counts against the binding energy. The binding energy, the energy required to remove the corresponding electron from its bonded state, allows the identification of the element since different elements and bonds have different binding energies [45]. Figure 2.5 depicts the setup of the XPS including the positioning of sample, X-ray, analyser (detector) and ion gun.
XPS is used in silicon nitride characterisation for determining the elemental composition of the film. For example, the amount of silicon, nitrogen, oxygen atoms, or the presence of impurities, but in particular to determine the silicon-to-nitrogen ratio [13, 16]. The amount of hydrogen can not be measured using XPS because the it has only a valence electron, which does not participate in chemical bonding. As such it cannot be distinguished from other element's valence electrons [46]. Aside from hydrogen and helium, all other elements can be measured [44]. Combined with ion-beam etching, which removes the surface atoms from the sample, a depth-profile of the sample can be obtained as well.

3
Methods

This chapter addresses the methods implemented to investigate the PECVD process factors and find an optimised PECVD recipe for silicon nitride deposition. First, the DoE creation is explained and the method of optimal recipe prediction is presented, then the experimental process flow described, and finally some methodological limitations are discussed.

3.1 Design of Experiments

In this work, six PECVD factors are investigated regarding their effects on silicon nitride thin films: pressure, RF power, frequency operation mode, and the gas flow rates of silane, ammonia, and nitrogen. These factors have been reported to affect silicon nitride deposition and film properties as discussed previously (see Chapter 2.2.1) and are tunable by the user of the PECVD tool. While temperature, both deposition and as a second step post-deposition annealing temperature, is another factor of potential interest, it is not included in this experimental work. The reason for that being, that adding another factor to the investigation would require a larger number of experimental runs which is limited by the available six-month time-frame for the thesis work.
The responses investigated are the refractive index of the SiN film at 1550 nm, the extinction coefficient at 550 nm, and the thickness uniformity of the deposited film. The wavelength of interest is 1550 nm, typical for telecom applications. However, the extinction coefficient is considered at 550 nm, because the obtained extinction coefficient values are larger at that wavelength and thus, more likely to be within the accurate measurement capability.
The optimal DoE for the investigation and optimisation of PECVD process parameters is created using the statistical discovery software JMP Pro 18.0.2 (Student Edition). The frequency mode is added to the design as a categorical factor with three levels corresponding to the three available levels of the PECVD tool used: low frequency (LF) at 100 kHz, high frequency (HF) at 13.56 MHz, and mixed frequency (MF). The remaining five factors are included in the design as continuous factors with three levels each, as depicted in Table 3.1. The decision to include three levels for the continuous factors is due to expectations that PECVD settings at intermediate level may be more favourable, or rather settings at very low or high values might be detrimental to the quality of the deposited SiN film. Furthermore, the factor settings of the default PECVD recipe available in the cleanroom (Myfab Chalmers) lie in the intermediate range. The only exception to this is the ammo-

nia flow rate. Here, some of the recipes with ammonia gas flow rate are unfeasible because of too high power reflection resulting in a tool error. Thus, the ammonia gas flow rate is adapted to higher values ranging from 2.5–10 sccm, for the recipes in questions. The corresponding model is a complete quadratic model including

Table 3.1: The three levels for each of the PECVD factor settings used in the DoE. LF, MF, and HF stand for low, mixed, and high frequency, respectively.

Factor	Type	Low level	Intermediate level	High level
Pressure (mTorr)	continuos	650	1275	1900
Power (W)	continuos	20	60	100
Frequency mode	categorical	LF	MF	HF
Silane flow rate (sccm)	continuos	100	295	490
Ammonia flow rate (sccm)	continuos	0	22.5	45
Nitrogen flow rate (sccm)	continuos	100	850	1600

the main factor effects, the quadratic effects displaying any curvature presents in the response-factor relationship, all two-factor interaction effects, and the intercept. The I-optimality criterion is chosen as design criterion to minimise the prediction variance. The number of random design starts, to ensure the global optimal design is found rather than a local one, is specified as 100000. The number of runs is defined as 38, which is above the minimum number of runs suggested for the specified design setup. An overview of all 38 PECVD factor combinations (recipes) making up the experimental design is available in Table A.4 in the Appendix.

3.2 Prediction of Optimal Recipes

The prediction of the best recipe is performed, once all the measured responses from the deposited silicon nitride samples have been obtained and added to the table containing the PECVD factor settings. The "Fit Model" option in JMP is used to fit a standard least squares model. The refractive index, the extinction coefficient and the thickness standard deviation are defined as y-variables, while all six main effects, the quadratic effects and two-factor interaction effects are added as model effects.

The prediction profiler is used to predict the optimal PECVD factor setting combinations. It is a graphical interface visualising the effect of changing one factor on the relationship between the process factors and responses being investigated and it is found in the least squares fit report in JMP [40]. For this, the desired responses are defined and the resulting desirability functions are maximised. For the refractive index the desirability is set to match a target of 2.0, while extinction coefficient and thickness deviation are to be minimised. In the desirability settings all three responses were assigned an equal importance value. This prediction process via the maximising of the desirability functions is repeated multiple times, resulting in multiple optimal recipes being predicted that are shown in Table 3.2 below.

Table 3.2: Predicted optimal PECVD recipes from which silicon nitride samples are fabricated. LF, MF, and HF denote low frequency, mixed frequency, and high frequency mode, respectively. The default PECVD recipe is listed for comparison.

Recipe ID	Pressure (mTorr)	Power (W)	Frequency Mode	5 % SiH4 (sccm)	NH3 (sccm)	N2 (sccm)
1 (default PECVD)	1250	40	LF	400	20	900
53	1710	100	HF	490	17	1599
54	1227	60	MF	100	6.6	850
55	900	64	LF	219	0.5	1523
58	1062	23	HF	397	43.5	100
76	1267	20	HF	490	32	1600
77	650	36	LF	427	4.8	1600
78	1275	60	HF	100	16.3	100
79	650	36	LF	490	8.6	1600

3.3 Process Flow for SiN Deposition

The process flow for the fabrication of silicon nitride samples is explained in the following. It is depicted in Figure 3.1 and consists of wafer cleaning, followed by the deposition of silicon nitre film in via PECVD, ellipsometer measurements, and partly XPS measurements. Fabrication and ellipsometer measurements are carried out at the Nanofabrication Laboratory Myfab Chalmers. The XPS measurements are performed at the Materials Processing Lab at Chalmers University of Technology with the assistance of Eric Tam.

The substrate used for the silicon nitride films are 4" (100 mm diameter) single-side-polished silicon wafers with the orientation <100>, a thickness of 525 µm, and p-type boron doping, from the company Silicon Materials. Before starting with the film deposition, the silicon wafers are cleaned following the standard clean (RCA cleaning procedure). Hereby, the wafers are first put into the SC-1 bath containing 1 L ammonium hydroxide (HN_4OH), 1 L hydrogen peroxide (H_2O_2) and approximately 5 L deionised water for 10 minutes at 80°C. This step removes the organic contaminants. The wafers are then rinsed in deionised water before being submerged in a hydrofluoric acid bath for 30 seconds to remove the native oxide layer, and then rinsed again in deionised water. After this, the wafers are submerged for another 10 minutes at 80-85°C in the SC-2 bath containing 1 L hydrochloric acid (HCl), 1 L hydrogen peroxide (H_2O_2) and approximately 5 L deionised water. This final cleaning step removes any metallic contaminants.

After cleaning, the silicon nitride film can be deposited using PECVD. The Oxford PlasmaPro 100 PECVD system is used at a wafer stage temperature of 300°C. The gases used during silicon nitride deposition are nitrogen (N_2), ammonia (NH_3), and 5 % silane (SiH_4) diluted in nitrogen. The PECVD recipe settings like pressure, RF power, frequency operation mode and gas flow rates are changed as part of the investigation. Pressure was set between 650–1900 mTorr, RF power varied from 20–100 W, silane flow rate from 100–500 sccm, ammonia flow rates from 0-45 sccm,

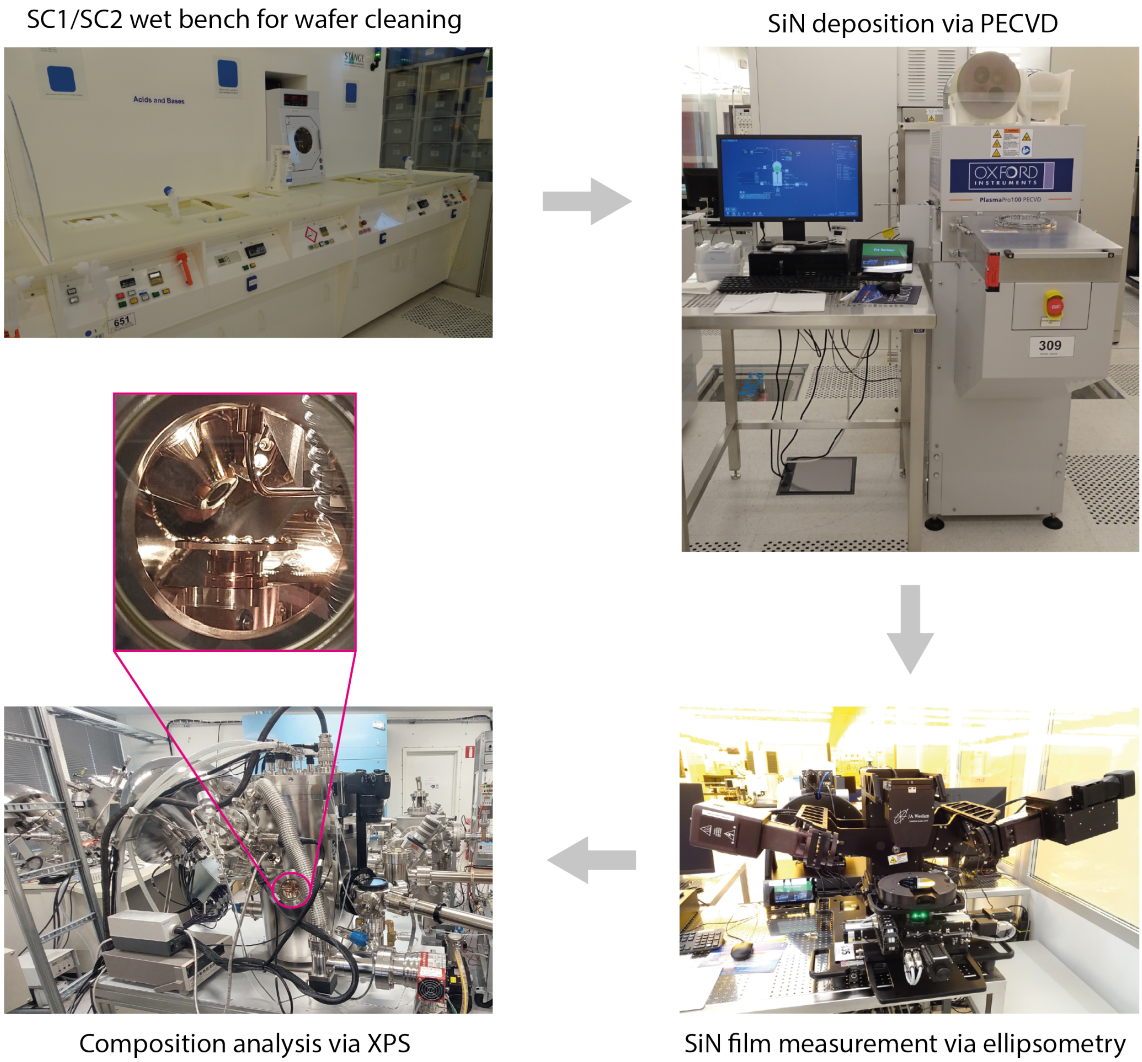

Figure 3.1: Illustration of the tools used during the process flow for silicon nitride deposition and subsequent measurements.

and nitrogen flow rates from 100–1600 sccm. Three different frequency operation modes for the RF power application are used: low frequency (LF) at 100 kHz, high frequency (HF) at 13.56 MHz, or mixed frequency (MF), which alternates between LF and HF mode. An approximately 100 nm thick SiN film deposition is aimed at. However, since the PECVD settings are varied, leading to the film thickness being unknown in advance, the deposition time is kept constant at 5 minutes and 43 seconds (for LF and HF operations). Recipes using the MF mode had a total of 18 cycles of alternating LF and HF deposition for 9 seconds each. Finally, the deposited silicon nitride film is measured using the RC2 ellipsometer from J.A. Woollam. Measurements are taken in a wavelength range from 500–2500 nm, at angles of 65°, 70°, and 75°, and at 39 points across the wafer. In the CompleteEASE software for the ellipsometer, the sample is modelled as a stack of three different material layers: the silicon substrate, a very thin (< 1 nm) native oxide layer, and then on top the silicon nitride layer, whereby a Tauc-Lorentz oscillator is used [47]. Refractive index values and extinction coefficient values for the samples are noted down

at 1550 nm and 550 nm, respectively. Average values are computed for the three responses from the 39 measurement points across the wafer, excluding points identified as outliers with respect to their MSE. For some samples X-ray Photoelectron Spectroscopy (XPS) measurements are performed using the PHI 5000 VersaProbe III Scanning XPS Microprobe. The X-ray source used is a monochromatic Al X-ray with an energy of 1486.6 eV and a beam size diameter of 100 µm. Survey scans ranging from 0–1350 eV at 1.0 eV increments are performed, to evaluate the overall elemental composition of the SiN film. The energy resolution of the 100 µm beam is 0.68 eV Ag3d5/2 peak from a sputter-cleaned Ag foil. The energy scale calibration is performed according to ISO15472 and the system aligned with Au (83.96 eV), Ag (368.21 eV) and Cu (932.62 eV). A carbon peak at $C1s = 284.8$ eV, is used as reference peak prior to qualitative analysis. The elemental composition is collected at the surface and after 10 minutes of Argon Ion (Ar+) sputter cleaning using 1 kV, 7 mA and a 3x3 mm^2 beam spot directed near the sample centre.

3.4 Limitations

In this section, the limitations of the chosen method are discussed. This includes the detection limit and measurement errors of the spectroscopy ellipsometer, as well as choices made in the experimental design.

3.4.1 Ellipsometer Sensitivity

In terms of resolution the ellipsometer can accurately measure changes is Ψ andΔ down to at least 0.02° and 0.1°, respectively [48]. However, it is not straightforward to estimate the exact error for derived quantities because it depends on several factors: the statistical errors of measurement data, systematic errors due to the use of incorrect models, and mathematical fitting errors. The statistical measurement errors are reported, while the systematic error is unknown but is attempted to be reduced by achieving a low MSE. As for fitting errors, they are only reported for the fit parameters, which includes film thickness, but not the derived quantities like refractive index and extinction coefficient. This makes it difficult to obtain the error in refractive index and extinction coefficient measurements.

Therefore, the accuracy and sensitivity of ellipsometry reported in literature is considered. Thickness measurements are reported to be accurate to 0.1-0.2 nm, making ellipsometry a highly sensitive tool to changes in thickness and well suited for the level of accuracy required for the film thickness in this work. However, when it comes to the measurement of the extinction coefficient, the ellipsometer is unable to measure very low values below $k = 1 \times 10^{-3}$ [41, 49]. Thus, measurement data below this sensitivity limit cannot be trusted to reflect the reality, as the values may simply be a result of noise. Nevertheless, a classification into values with higher extinction coefficient $k > 1 \times 10^{-3}$ and lower extinction coefficient $k < 1 \times 10^{-3}$ is possible.

3.4.2 Experimental Design Choices

Regarding the DoE, some design choices are made to keep the number of experimental runs within the manageable capacity. In particular, blocking factors and repeated runs are not included, which may limit the collected data's accurate representation of the real picture. Blocking factors can be used to account for sources of variability in the experiment. This helps to reduce noise in the experiment. For example, they are typically used when experimental runs are performed on different days to account for the day-to-day variability, if runs are performed by different operators, or different material batches are used [38]. The use of blocking factors has been considered in this work, and could be useful since day-to-day variability might be present due to shared use of the machine over multiple weeks, whereby silicon nitride is not the only material deposited in the PECVD chamber. However, upon creating a DoE including blocking factors based on a pre-determined deposition schedule, the number of experimental runs required increases compared to the design without blocking factors. Due to the limited time budget, as well as finding similar metrics in terms of design evaluation criteria such as prediction variance, power analysis, efficiency, and relative error of standard estimates, for the proposed 38-run design and an alternative design with blocking factors, the design without blocking factors is chosen. For similar reasons, repetitions of all the experimental runs are not inherently planned for, as this would require significantly more time. This decision is made in favour of using the available run budget for investigating as many PECVD factors of interest as possible.

4
Results

In this chapter the measurement results of the silicon nitride films corresponding to the designed experiment are presented, the most important factors and trends of the PECVD process are identified, and the prediction performance of this optimisation approach is discussed.

4.1 Significant Factors & Trends

One of the goals in this thesis work is to identify the significant factors (i.e. process parameters) of the PECVD process for silicon nitride deposition, as well as any correlations and interaction effects between different factors or responses. Therefore, the measured responses of interest, namely the thickness uniformity of the deposited silicon nitride layer across the 100 mm wafer, the refractive index and the extinction coefficient, are analysed.
By performing a standard least squares fit of the full quadratic model (see Chapter 3.1) to the measured data in JMP, significant model effects, i.e. effects of PECVD factors or their interactions, are determined. Effects are classified as statistically significant for each investigated response, if the p-value reported for the effect tests is < 0.05. A small p-value indicates the results obtained are unlikely to be random. The effect tests check the null hypothesis, i.e. if for each effect specified in the chosen model, all the parameters associated with that effect are zero. In JMP the F-test is used for effect tests, evaluating whether a (process) factor has a statistically significant impact on the investigated response [40].
The measured data for the 38 experimental PECVD runs are presented in Table 4.1 and the results of the effect tests can be found in the Appendix.
Upon performing a multivariate analysis in JMP, no strong correlation (correlation coefficient > 0.7) is found. There is only a moderate correlation ($r = -0.51$) between ammonia flow rate and the refractive index. The lack of direct relations between PECVD process parameters and investigated responses has been mentioned in other investigations as well [15, 30]. This may be a result from the presence of two-factor interactions in the PECVD process, which will be discussed in more detail throughout this chapter. Nevertheless, some trends equating to weaker correlations can be observed, which are addressed individually for each response in the following sections, alongside the significant effects present.

Table 4.1: Measurement data of the SiN films deposited according to the 38 PECVD recipes of the DoE. It contains the standard deviation of thickness across the 4"-wafer relative to the average thickness, the refractive index n at 1550 nm, the extinction coefficient k at 550 nm, and the compositional silicon-to-nitrogen ratio.

Recipe ID	Thickness Std. Dev. (%)	n at 1550 nm	k at 550 nm	Si/N
15	64.60	2.211	5.8E-03	/
16	1.05	1.938	1.0E-03	/
17	2.23	1.932	9.6E-05	/
18	0.39	2.164	3.5E-02	/
19	3.33	1.794	1.6E-04	/
20	17.54	1.934	3.9E-03	/
21	2.99	1.811	7.7E-04	/
22	5.67	1.977	6.2E-03	/
23	1.15	2.047	1.2E-02	1.09
24	3.40	1.829	1.8E-03	/
25	0.68	2.836	1.2E-03	2.46
26	3.07	1.810	2.5E-09	/
27	1.10	1.976	1.2E-03	/
28	1.47	1.861	1.0E-03	/
29	0.25	1.870	2.4E-03	/
30	0.98	1.943	1.2E-03	/
31	5.79	1.868	5.0E-04	/
32	7.65	1.962	7.7E-04	/
33	0.34	2.624	1.1E-01	2.22
34	0.76	1.866	3.0E-08	/
35	3.03	1.829	4.5E-04	/
36	0.52	1.763	7.1E-04	/
37	1.22	1.851	3.1E-04	0.71
38	0.11	1.858	1.7E-03	/
39	0.25	1.869	1.1E-03	/
40	103.53	1.900	1.3E-03	/
41	1.19	2.250	4.4E-01	/
42	0.35	1.870	5.6E-04	/
43	0.65	1.788	8.0E-05	0.74
44	5.03	1.801	3.7E-04	/
45	0.74	1.899	1.6E-03	/
46	0.75	2.425	6.6E-02	/
47	0.80	2.877	1.9E-01	/
48	0.49	2.599	9.3E-02	/
49	0.63	1.933	4.8E-05	/
50	0.89	1.864	1.8E-04	/
51	3.04	1.914	2.4E-04	/
52	2.71	1.776	7.6E-05	/

4.1.1 Refractive Index

The refractive index of the deposited silicon nitride layer seems to be significantly affected by five of the six PECVD process factors. The pressure level does not significantly affect the refractive index of silicon nitride layer during PECVD deposition, contrary to other reports [15]. However, the power, frequency mode, ammonia, silane and nitrogen gas flow rates do affect the refractive index.
Especially the gas flow rate of ammonia affects the refractive index of the silicon nitride layer. A lower ammonia gas flow rate relative to the silane gas flow rate seems favourable for achieving a higher refractive index as can be seen in Figure 4.1. The reason for that is that at lower ammonia gas flow rates less nitrogen atoms are incorporated as the silicon nitride layer forms, because the gaseous, reactive nitrogen is not as quickly replenished at lower gas flow rates [34]. he variation in refractive index values at identical gas flow ratios arises from differences in other PECVD process parameters.

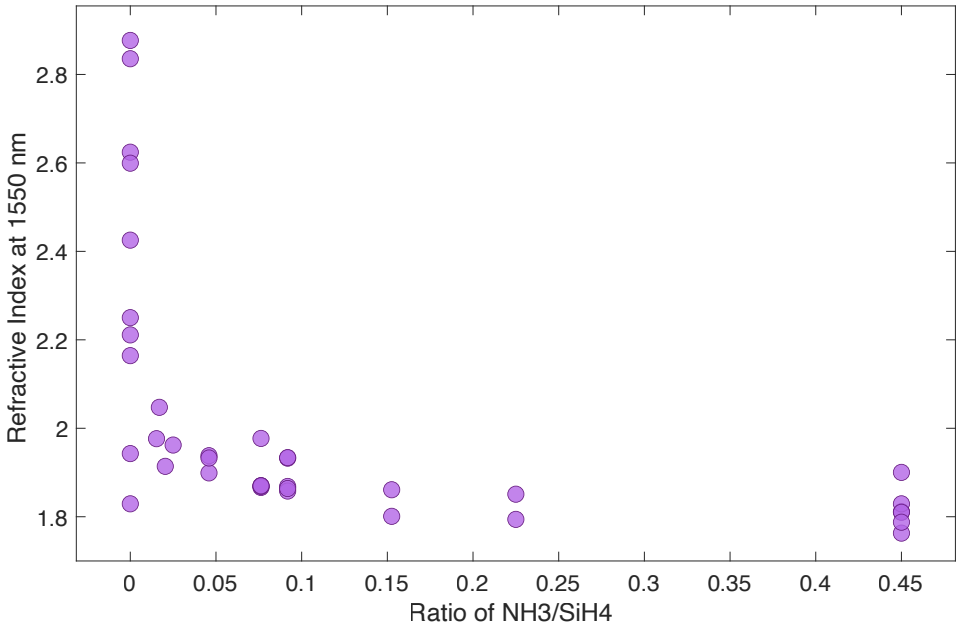

Figure 4.1: Observed relationship between refractive index and ratio between the gas flow rates of ammonia and silane precursor gas.

This gas flow ratio-dependent behaviour, and the resulting relationship of a higher silicon-to-nitrogen ratio resulting in a higher refractive index, is well supported by literature [15, 28, 32, 34, 36]. XPS measurements of a subset of deposited SiN films indicate this relationship too, as shown in Figure 4.2.
Furthermore, there are many relevant two-factor interactions affecting the refractive index, including all six PECVD factors. The exact significant effects are listed in Table A.1 in the Appendix. These two-factor interactions have the effect that the influence of one PECVD factor on the refractive index changes depending on the setting of another factor. For example, decreasing the gas flow rate of ammonia or nitrogen enhances the positive relationship between silane flow rate and refractive

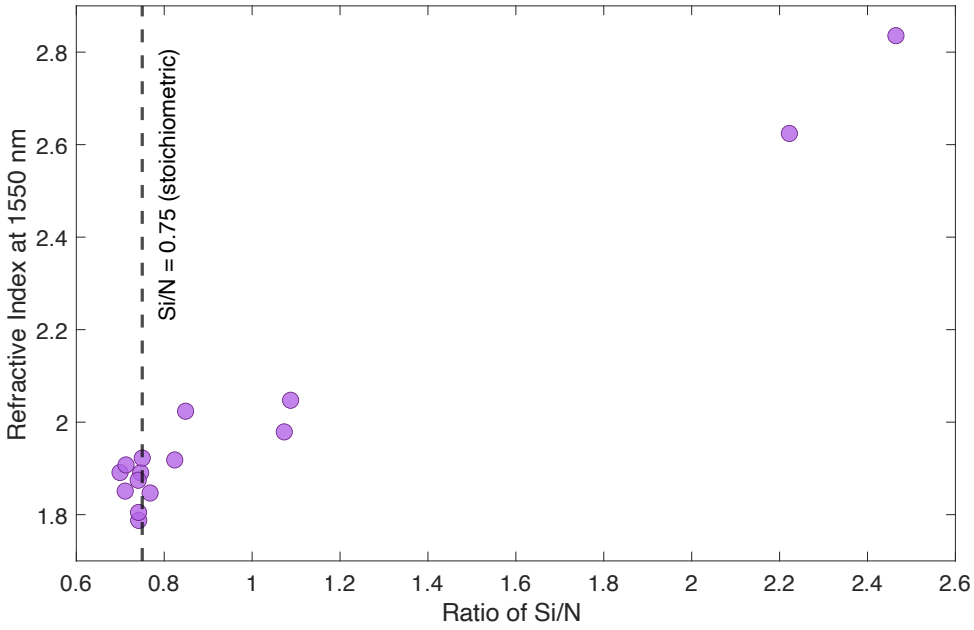

Figure 4.2: Observed relationship between refractive index and elemental silicon-to-nitrogen ratio of a selection of the deposited silicon nitride films.

index. The frequency also influences how strongly the refractive index is affected by the ammonia gas flow rate. At high frequency operation mode the relationship between the two is much steeper. The largest refractive index values (up to $n = 2.8$ at 1550 nm) in this experiment are achieved using high frequency mode. Additionally, the statistical significance of the quadratic effect of the ammonia flow rate indicates that there is some curvature in the relationship between ammonia flow rate and refractive index.
Overall, the ammonia gas flow rate seems to be the most important factor to consider for the refractive index of a silicon nitride film deposited via PECVD, with a low ammonia gas flow rate favourable for achieving higher refractive indices. The choice of frequency operation mode and silane gas flow rate can enhance this relationship further.

4.1.2 Extinction Coefficient

For the extinction coefficient, which relates to absorptivity of the silicon nitride layer, some trends with the refractive index and the ammonia gas flow rate can be observed. PECVD process parameters with statistically significant impact on the extinction coefficient are the frequency mode used, the ammonia gas flow rate, and the nitrogen gas flow rate according to analysis of the experimental data.
It is not surprising that ammonia flow rates affect the extinction coefficient. Ammonia flow rates are known to influence the absorption of the silicon nitride film because of the N-H bonds acting as absorption centres at telecom wavelengths [10, 11]. Higher ammonia flow rates lead to a greater number of nitrogen atoms being incorporated into the deposited layer since nitrogen is replenished more quickly in the

reaction chamber. As a result, more N-H bonds form too [15]. While the ammonia gas flow rate is determined as statistically significant, there is no clear trend observed from the collected data. A reason for that could be that many of the extinction coefficients (k-values obtained at 550 nm) are below the measurement sensitivity limit ($k \approx 10^{-3}$) of the ellipsometer. Therefore, any relationship that is potentially present between the process factors and low extinction coefficients is not identifiable from the collected data. Thus, one can only distinguish between high ($k > 10^{-3}$) and low ($k < 10^{-3}$) extinction coefficients. However, it can be seen in Figure 4.3 that a very low ammonia gas flow rate, close to zero, tends to result in high extinction coefficient values. This result is not in agreement with reports of NH_3-free silicon nitride layers resulting in less absorption losses [6, 13, 15]. This might be a result of different settings used for the remaining PECVD process parameters, or the use of alternative PECVD methods. Alternatives like inductively-coupled plasma chemical vapour deposition (ICPECVD) or electron cyclotron resonance plasma-enhanced chemical vapour deposition (ECR-PECVD) can achieve dissociation of N_2 due to the higher concentrated plasma and are reported to lead to lower hydrogen content present in deposited SiN films than capacitively coupled, parallel plate PECVD machines [6, 13].

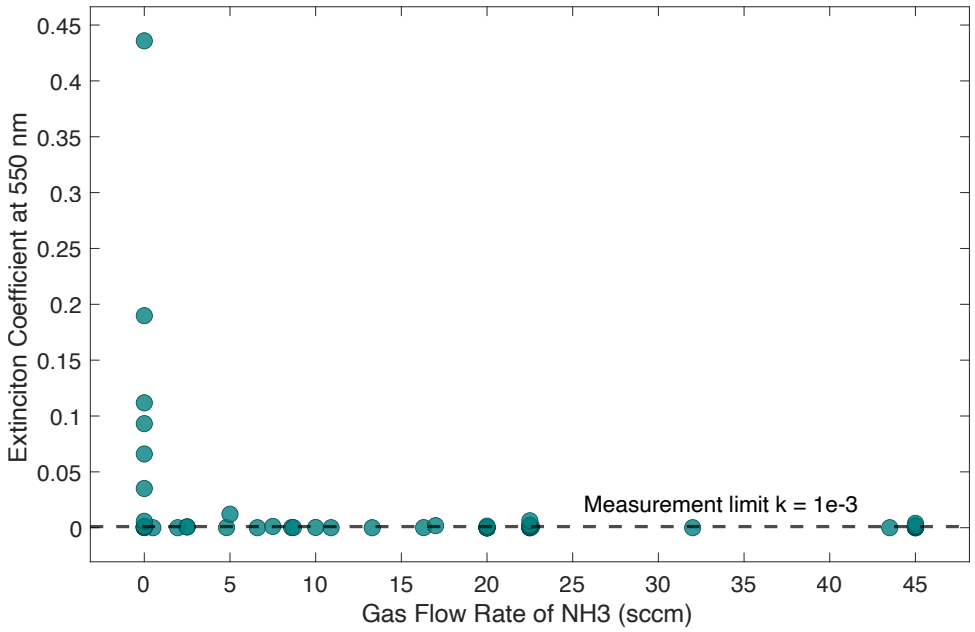

Figure 4.3: High extinction coefficient values appear at very low ammonia gas flow rates.

As for the influence of the frequency mode, it can be observed that the high frequency setting results in silicon nitride layers with the highest extinction coefficient values, while all low frequency recipes result in an extinction coefficient $k \leq 0.001$. Similarly, the high extinction coefficients are observed more often at low nitrogen gas flow rates (100 sccm), while medium flow rates (500-900 sccm) seem more favourable. It has to be noted, that the majority of the SiN samples have an extinction coefficient below

the accurate measurement limit regardless of the frequency mode or nitrogen gas flow rate used. The few points outside this range are not a large enough data set to be confident in establishing that these are not just outliers. Therefore, the data from the 38 different SiN samples is not sufficient to draw any clear conclusions about trends with regard to the influence of nitrogen gas flow rate and frequency mode on the absorptivity of the deposited SiN film. Thus, further investigation is required to establish confidence in observed trends and provide reasonable explanations.
In addition to the influence of PECVD process parameters, a correlation between the extinction coefficient and the refractive index is found. Figure 4.4 shows the relationship between these two responses.

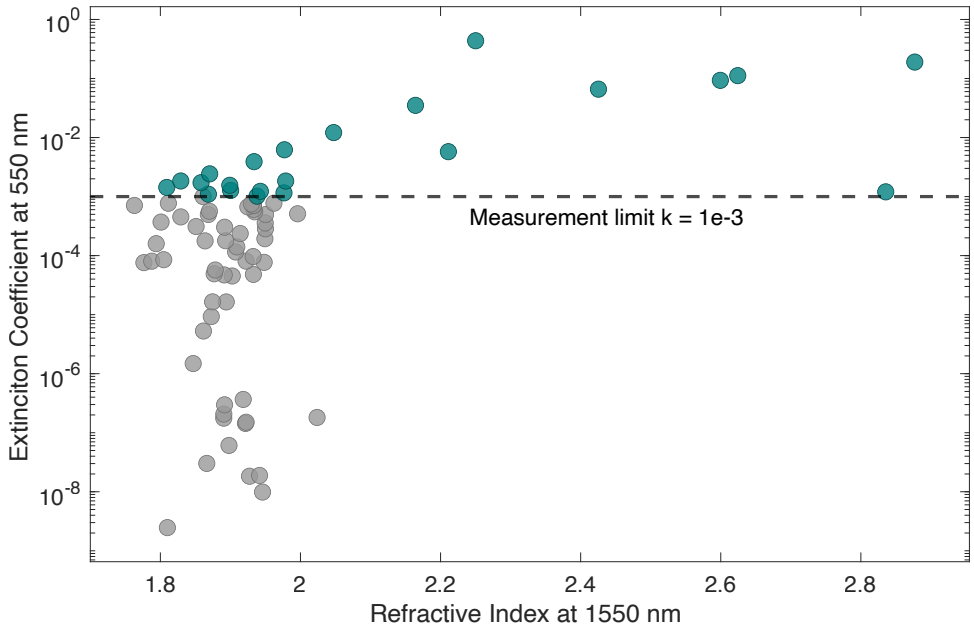

Figure 4.4: Positive correlation between refractive index and extinction coefficient for values above the measurement limit.

It can be seen that there is some positive correlation between the refractive index and the extinction coefficient of the silicon nitride film. While a large part of the silicon nitride samples have a extinction coefficient below the measurement limit and thus, do not show a clear trend with regard to the refractive index, it can be seen that the highest extinction coefficients occur together with the highest refractive index values. A similar trend has been reported for absorption losses in silicon nitride waveguides. Absorption losses have been found to increase for silicon-rich silicon nitride waveguides and silicon-rich SiN layers have a higher refractive index than stoichiometric SiN films [28, 50]. Therefore, it seems plausible that a higher extinction coefficient, indicative of the film's absorptivity, is found in relation with a higher refractive index.
To summarise, the factors ammonia and nitrogen gas flow rate, and the frequency mode selected for the PECVD silicon nitride deposition process impact the extinction coefficient significantly. Additionally, a positive correlation between extinction

coefficient and refractive index can be observed, indicating higher absorption of the silicon nitride films for silicon-rich films.

4.1.3 Thickness Uniformity

The thickness uniformity of the deposited silicon nitride layer across the wafer is most clearly influenced by the frequency mode. The frequency mode is the only statistically significant main effect of the six PECVD factors investigated. Figure 4.5 shows that high frequency recipes give the best thickness uniformity. Low frequency recipes on the other hand show the highest deviations regarding thickness uniformity. Pressure also seems to have an impact, but only insofar as that the highest pressure setting used (1900 mTorr) results in a few silicon nitride films with considerably worse thickness uniformity than the rest of the samples. These films with bad uniformity had standard deviations relative to the average film thickness of the order of 18 %, 65 %, and even 104 %.

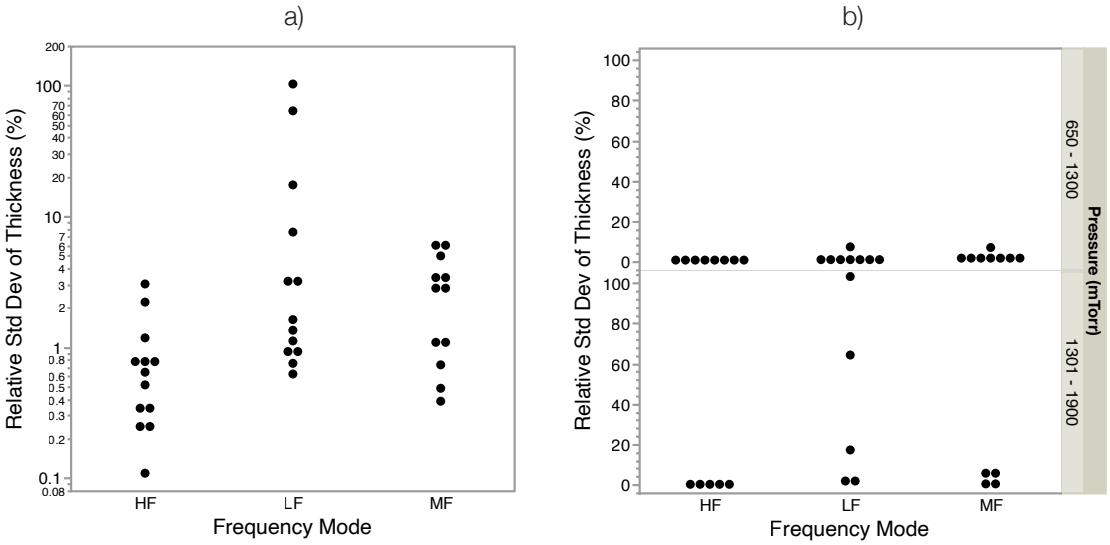

Figure 4.5: Relative standard deviation of film thickness with respect to the average film thickness of the 38 silicon nitride samples fabricated with various PECVD settings according to the DoE. a) Relative thickness standard deviation depending on frequency mode. b) Thickness deviation relation with frequency mode changes at different chamber pressure levels due to two-factor interaction effects between frequency mode and pressure.

Furthermore, there are two-factor interactions that appear to be statistically significant (see Table A.2 in Appendix). The interaction between silane and ammonia gas flow rates, as well as between RF power, pressure and those two gas flow rates seem to have a significant effect on the thickness uniformity. These two-factor interactions influence how strongly one factor affects the impact of another factor on the responses. For example, Figure 4.5 shows that at low pressure setting (650 mTorr) the choice of frequency mode does not seem to affect the thickness uniformity strongly. However, at high pressure setting (1900 mTorr) the low frequency mode had an undesirable impact on the thickness uniformity in some cases.

Similarly, at low pressure setting the silane and ammonia gas flow rate seem irrelevant as the relative thickness uniformity is below 3 % throughout, while at high pressure there are distinct unfavourable silane and ammonia gas flow rate combinations for achieving a uniform SiN film thickness. In general, the best thickness uniformity is achieved at high silane gas flow rates (500 sccm) and medium to low ammonia gas flow rates. This is depicted in Figure 4.6.

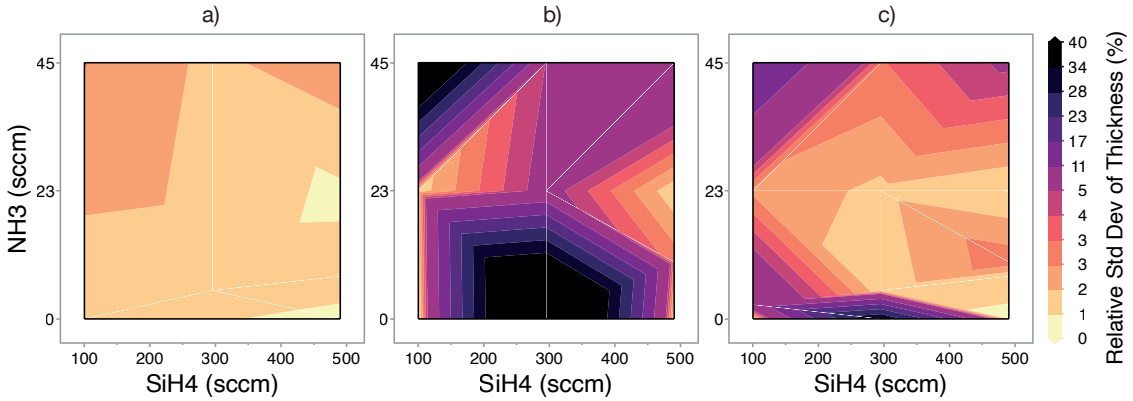

Figure 4.6: Relative standard deviation of film thickness with respect to the average film thickness of the silicon nitride samples fabricated with various PECVD settings according to the DoE. a) At 650 mTorr chamber pressure. b) At 1900 mTorr chamber pressure. c) Influence of silane and ammonia gas flow rates on the relative thickness deviation taking into account all 38 samples.

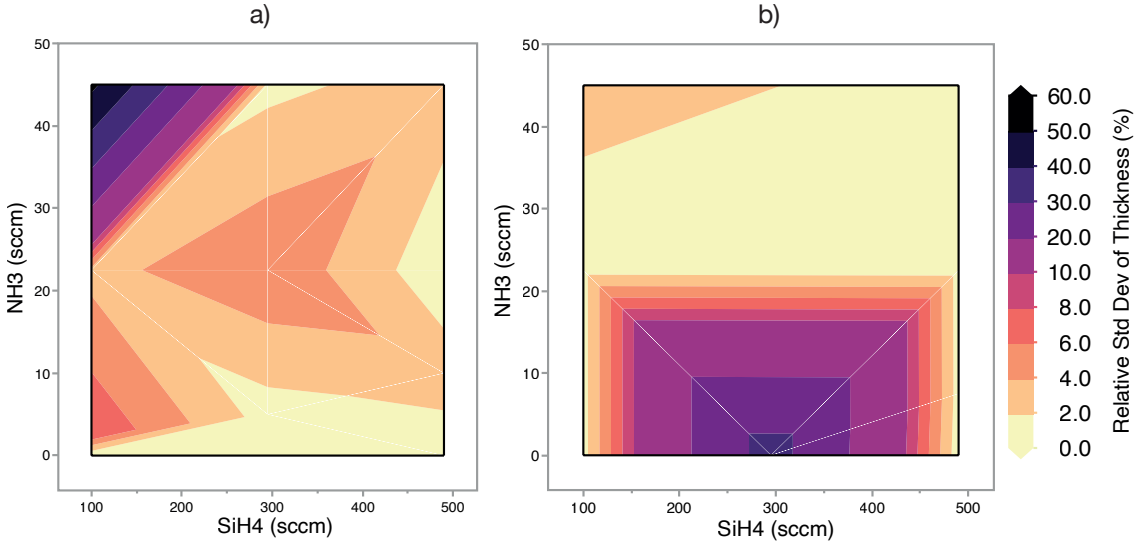

Figure 4.7: Relative standard deviation of film thickness with respect to the average film thickness of the silicon nitride samples fabricated with various PECVD settings according to the DoE. a) At 20 W RF power. b) At 100 W RF power.

As for the two-factor interaction effects involving power, Figure 4.7 shows how the favoured gas flow rates of silane and ammonia vary depending on the RF power

setting. At low power (20 W) setting, high ammonia and low silane gas flow rates result in the worst thickness uniformity. As the power increases to 100 W this relationships changes and medium to high gas flow rates for ammonia appear most favourable, regardless of the silane flow rate.
Overall the presence of these two-factor interactions illustrates the difficulty in finding the optimal factor combination in the PECVD process, as changing one factor setting changes the impact of other factors on the responses being investigated. The presence of interaction effects between the PECVD process factors and the difficulty in finding consistent trends, that can be used as rule of thumb, is found in other optimisation studies too [30]. This suggests that PECVD is indeed a process with complex relationships between process factors and resulting film properties, where perhaps methods like optimal design of experiment are very useful, or even necessary, for the optimisation according to the individual objective.
It can be concluded that the choice of frequency mode is the most important factor setting when it comes to thickness uniformity. In addition, according to the data collected in this thesis work, there are two-factor interactions that affect the thickness uniformity of the silicon nitride layer during deposition.

4.2 Predicted PECVD Recipes

The main goal in this thesis is to optimise the PECVD process parameters to arrive at a setting combination that gives the best responses: specifically, a silicon nitride layer with good thickness uniformity, a refractive index comparable to stoichiometric or LPCVD-deposited silicon nitride, and a small extinction coefficient, i.e. low absorption at wavelengths of interest. In the following section the performance of the used method, namely using the prediction profiler in JMP based on data collected according to the design of experiment, to predict optimal recipes, is evaluated.

4.2.1 Predicted Recipes & Resulting SiN Films

The predicted silicon nitride PECVD recipes are evaluated in terms of how well the desired responses (a refractive index close to two, a minimised extinction coefficient, and good thickness uniformity) are accomplished. Additionally their performance is compared to the default LPCVD and the default low frequency PECVD recipes. Overall, most of the predicted recipes lead to the deposition of good silicon nitride layers, but reaching the desired target for all three responses simultaneously, seems to prove difficult.
Table 4.2 shows the measured results for the predicted PECVD recipes as well as the default LPCVD and PECVD recipes.
In terms of the extinction coefficient, all but one predicted recipe had values below or at the measurement sensitivity limit, and thus, are considered to have a low extinction coefficient as far as can be ascertained by the ellipsometer measurement. This puts the predicted recipes at least on equal par with the default LPCVD and default PECVD recipe in regard to the absorption of the silicon nitride layer. Regarding the thickness uniformity of the predicted recipes, none showed vast variations in

Table 4.2: Measurement data of the SiN films deposited according to the predicted optimal PECVD recipes and the default LPCVD and PECVD recipes. It contains the standard deviation of film thickness across the 4"-wafer relative to the average thickness, the refractive index n at 1550 nm, the extinction coefficient k at 550 nm, and the compositional silicon-to-nitrogen ratio.

Recipe ID	Thickness Std. Dev. (%)	n at 1550 nm	k at 550 nm	Si/N
0 (default LPCVD)	0.61	1.996	5.1E-04	0.74
1 (default PECVD)	2.11	1.891	7.3E-05	0.74
53	0.37	1.979	1.8E-03	1.07
54	1.35	1.847	1.5E-06	0.77
55	4.61	2.024	1.8E-07	0.85
58	0.33	1.918	3.7E-07	0.82
76	0.19	1.875	1.6E-05	0.74
77	2.76	1.922	8.1E-05	0.75
78	0.84	1.805	8.5E-05	0.74
79	3.08	1.907	1.2E-04	0.71

silicon nitride layer thickness across the 4" wafer. Five out of eight predicted recipes result in a better thickness uniformity than the average thickness uniformity of the default PECVD recipe, while another recipe had a similar thickness deviation. Compared to the silicon nitride film deposited by LPCVD, three predicted recipes improved the thickness uniformity even further. Considering the refractive index, five predicted PECVD factor setting combinations performed better than the default PECVD recipe. However, only two recipes achieved a refractive index close to two with $n = 2.024$ and $n = 1.979$, with the second being the closest to the LPCVD SiN refractive index of $n = 1.996$.

Looking at all three responses at the same times, makes it more difficult to decide on the best overall recipe. The reason for this being that an improvement in one response seems to result in a deterioration of at least one of the other two responses. For example, recipe 53, which has a very good refractive index, has a worse extinction coefficient. This observation is in accordance with correlation between refractive index and extinction coefficient mentioned previously. Perhaps it is physically difficult to achieve a refractive index $n = 2.0$ and a very low extinction coefficient for silicon nitride films using PECVD. An analysis of the silicon nitride film composition via XPS measurements reveals that the PECVD deposited SiN films achieving a refractive index close to $n = 2.0$ are silicon-rich SiN films. Silicon-rich SiN films have a greater ratio of silicon atoms to nitrogen atoms in the silicon nitride layer compared to the stoichiometric Si/N ratio of 0.75. The two silicon nitride films with refractive indices of $n = 2.024$ and $n = 1.979$ have a Si/N ratio of 0.85 and 1.07, respectively. In contrast, the default LPCVD and PECVD silicon nitride films have a Si/N ratio of 0.74. While the default LPCVD silicon nitride film has a refractive index of $n = 1.996$, the default PECVD film has $n = 1.891$, even though they have the same Si/N ratio. The reason for this may be the different densities of the SiN films deposited via LPCVD or PECVD.

LPCVD films have a higher density than PECVD films, especially if capacitive

PECVD is used, like in this work, as opposed to higher quality methods such as ICPECVD or ECR-PECVD that result in less hydrogen incorporation [6, 13, 16]. This is because a higher concentration of hydrogen tends to be incorporated in the samples when using PECVD, resulting in a more voluminous atomic structure [16, 37, 51]. The mass density of the SiN film is often related to the refractive index measured, whereby a increase in refractive index is often associated with an increase in mass density. Therefore, silicon nitride layers with higher hydrogen concentration, and thus lower mass density, can have lower refractive indices than their higher density counterpart of same Si/N composition [37]. However, the composition of the film also affects the refractive index. The density of SiN films with close to stoichiometric Si/N ratio and the density of N-rich silicon nitride has been reported to be greater than that of Si-rich SiN films [27, 37]. This could explain why increasing silicon content does not result in higher refractive indices in all cases, since the refractive index is both density and composition dependent.
When focusing on a stoichiometric Si/N ratio of 0.75, instead of obtaining a refractive index $n = 2.0$, a predicted recipe that fulfils all three desired responses can be identified. Achieving stoichiometric silicon nitride films (Si_3N_4) is relevant because it has been reported to have the lowest hydrogen concentration and be favourable for low losses [15]. In this case, Recipe 76 represents the optimal choice, with a Si/N ratio close to the stoichiometric value of 0.75, a low extinction coefficient $k < 10^{-3}$, and a very good thickness uniformity according to the thickness standard deviation relative to the average thickness across the wafer being 0.19 % and the thickness map shown in Figure 4.8. This PECVD recipe results in a better thickness uniformity than both the default LPCVD and PECVD recipes, while achieving the same Si/N ratio and a similarly low extinction coefficient.

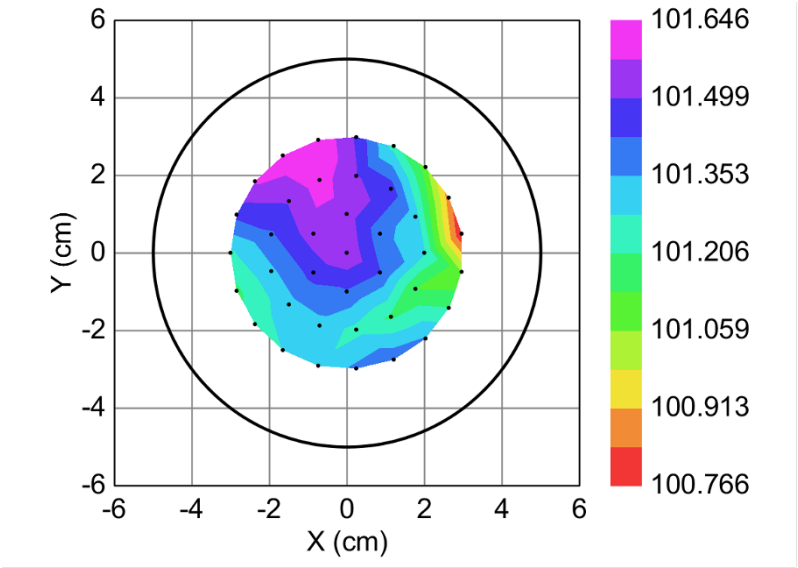

Figure 4.8: Depiction of the silicon nitride film thickness measured with the ellipsometer in a 39-point measurement for the predicted recipe (ID 76) with the best thickness uniformity.

To conclude, most predicted PECVD recipes for silicon nitride deposition perform well compared to the whole set of recipes tried throughout this work. Improvements in each of the three responses of interest, the refractive index, extinction coefficient, and thickness uniformity, are achieved compared to the default low frequency silicon nitride recipe. However, it seems that all three responses of interest, the refractive index, extinction coefficient, and thickness uniformity, cannot be optimised simultaneously to reach the desired targets. Nevertheless, when focusing on Si/N ratio instead of refractive index, a predicted recipe resulting in improved or equal responses to the default LPCVD and PECVD recipes is obtained.

4.2.2 Multiple Optimal Recipes

When using the prediction profiler in JMP to predict the optimal combination of PECVD process parameters settings for achieving a silicon nitride layer with the desired properties, multiple factor combinations can be found. This occurs as the desirability functions are repeatedly maximised. In some cases only minor changes to the different factor settings occur, in the order of single or decimal digits. However, upon changing the initial factor settings, i.e. specifying factor settings in the prediction profiler window, which deviate from the previously predicted optimal recipe, a different combination of "optimal" PECVD factor settings may be found. As a result, multiple optimal recipes can be predicted, whereby the number of predicted recipes seems to depend partly on the number of repetitions, at which different initial factor settings are chosen and the desirability functions maximised. These observations leads to two possible reasonings: either the multidimensional process parameter space contains multiple optima, or this is an artifact of the model and data that the prediction is based on.
The first option, that multiple optimal PECVD factor setting combinations exist, is a possibility. After all, silicon nitride formation via PECVD is a process influenced by multiple factors, exhibiting in part significant interaction effects, as shown by the results explained previously. As such, it is not an unfounded assumption that multiple solutions to the target optimisation problem exist in this multidimensional space. The second option is that predicting multiple recipes with the desired outcome is an artifact of the methodology and does not reflect reality. The choices made in the setup for the prediction profiler, but also the accuracy and precision of the measured responses could be a reason for this.

4.2.2.1 Prediction Profiler Settings

During the use of the prediction profiler in JMP, decisions regarding the definition of desirability functions, the inclusion or removal of non-significant effects, and the data set are made. These can affect the outcome of the predicted optimal PECVD recipe.
The way desirability functions are defined, affects the prediction results. As part of setting the desirability, i.e. the desired response, a low, middle, and high response value has to be specified. By defining these boundaries for the desirability functions, the acceptable range for the desired target response is defined. It is plausible that a broader desirability function results in more optima being found.

The model choice can also affect the number of optimal PECVD factor combinations found. For instance, the complete quadratic model specified for the experimental design can be used, or the model used for the prediction is reduced, by removing effects that are not overall significant (p-value > 0.01) and non-contained (insignificant main effects involved in significant two-factor interactions are not removed). There is no universal agreement as to which of these two options is the right approach. Leaving in all the model terms ensures that factor effects, which according to the statistical test applied are not significant but may still influence the outcome, are not neglected. However, including only significant effects in the model used for the prediction has the benefit of reducing the number of effects involved and thus, complexity.
Another aspect to consider is the conformance, or lack of it, between the different predicted recipes. Table 4.3 shows that predictions made based on solely the significant effects can result in a very different gas flow rate ratio compared to predictions involving all effects. Furthermore, the data set used for the prediction of the optimal PECVD factor setting combinations matters as well. Different results can occur when using only the 38 samples according to the experimental design, as opposed to using a 52-run data set, including additional samples from preliminary test runs and repetitions of some recipes. Normally, a greater data set is favoured when it comes to making predictions. Similar optimal PECVD recipes are found for both the 38-run and the extended data set (see Table 4.3), indicating that the 38-run DoE is sufficient, i.e. that no crucial information is added by the extra data. It is interesting to note though, that the size of the data set seems to matter more, when taking only the significant effects into account for the recipe prediction.

Table 4.3: Comparison of predicted PECVD recipes based on the 38 experimental runs according to the DoE and based on a 52-run data set containing additional repeated and preliminary runs. Recipes labelled with "all effects" included all model terms (factor effects) in the prediction, while for "only significant effects" recipes the non-significant (p-value > 0.01), non-contained effects are removed prior to the prediction of optimal PECVD factor settings.

Effects contained	Size of data set	Pressure (mTorr)	Power (W)	Frequency Mode	5 % SiH4 (sccm)	NH3 (sccm)	N2 (sccm)	SiH4/NH3
All effects	38	650	20	HF	490	45	1261	11
	52	650	20	HF	500	39	1000	13
All effects	38	650	20	LF	428	5.6	1600	76
	52	650	20	LF	384	4.7	1000	82
All effects	38	1275	20	HF	479	30.8	1600	16
	52	1275	20	HF	500	33	1682	15
Only	38	1275	36	HF	490	24.2	1600	20
significant	52	650	20	LF	262	1.3	1900	202
effects	52	650	20	LF	25	3.1	1900	8

In conclusion, the narrowness of the defined desirability functions, the choice of model and the size of the data set can affect the number of optimal recipes found and lead to different optimal PECVD factor settings. To ascertain, whether all predicted recipes actually result in a silicon nitride layer with the desired properties,

how to narrow down the selection of optimal recipes, and which approach regarding the prediction process is most suitable to reliably identify the best recipe, further investigation is required.

4.2.2.2 Reproducibility of Data

In addition to the chosen prediction setup, the accuracy of the measurement data is relevant as well when it comes to the prediction of the optimal PECVD recipe for silicon nitride deposition. If the measured data does not reflect the true reality, then the predicted factor setting combination for achieving the desired responses is unlikely to match the true reality either. Both the measurement accuracy and precision, as well as the reproducibility of the different PECVD recipes plays a role in this regard.
Especially for minimising the extinction coefficient of the SiN layer, this is an issue. Because a large part of the samples have an extinction coefficient below the reliable measurement sensitivity limit of the ellipsometer ($k < 10^{-3}$), the data is only valid for narrowing down which PECVD settings result in a high (above measurement limit) or low (below measurement limit) extinction coefficient. Truly finding the minimum extinction coefficient among the data set and the corresponding factor setting combinations is not possible with this measurement method. Considering the broader goal of developing the most suitable PECVD recipe for fabricating silicon nitride waveguides with minimised propagation losses, other characterisation methods are required. For example, propagation losses can be determined using the cut-back method by measuring transmission through waveguides of varying lengths, or by extracting loss from the intrinsic line-width or quality factor of micro-ring resonators [4]. However, this requires the fabrication of waveguides and thus, additional fabrication steps compared to depositing only the silicon nitride film. For a DoE involving numerous experimental runs, this can result in a considerable additional time demand.
Upon repeating some of the ellipsometer measurements three to eight times to estimate how reproducible the measured values are, some deviations in SiN film thickness and especially the extinction coefficient are observed. The reproducibility of the ellipsometer data seems to be very sample dependent and tends to become worse for those with higher MSE, where the model used for fitting does not match the actual deposited film well. The refractive index typically varies by 0.0006–0.05, the thickness at the centre point of the wafer changes by 0.02–6 nm, and the extinction coefficient shows variations in the range of 0.007–0.02 for samples with $k > 10^{-3}$ and otherwise remains below the measurement limit. Part of this deviation is due to the model fitting in the ellipsometer process, which leads to some error in the accuracy of the measured film properties in addition to the physical measurement error.
Beyond the measurement itself, the reproducibility of the tested PECVD recipes influence the prediction performance too. If the SiN film resulting from a recipe cannot be reliable reproduced, the measured responses vary significantly. Hence, the respective factor setting combination of that recipe cannot be relied on either, when making predictions about the responses. Figure 4.9 shows how the default PECVD recipe and two other recipes from the DoE perform in terms of reproducibility. The

refractive index is the most similar between the different repetitions, while the film thickness show deviations up to 17 nm. The obtained extinction coefficients appear to be within the same order of magnitude even though the values are slightly below the reliable measurement limit. It is noteworthy that the refractive index and film thickness data points clustered closely together tend to stem from samples that were deposited on the same day. The difference between samples fabricated on the same day and samples fabricated days to weeks prior, indicates the presence of day-to-day variability in the PECVD deposition process. This is not surprising, as the PECVD machine is used for deposition of other materials and undergoes maintenance in the meantime. This affects the conditions in the chamber like gas flow dynamics, precursor distribution, the plasma state, and contamination due to residues or inefficient pumping, because of process drifts or machine wear [52]. Prediction variance caused by this could be reduced by including blocking factors that help account for day-to-day variability in the experimental design [38].

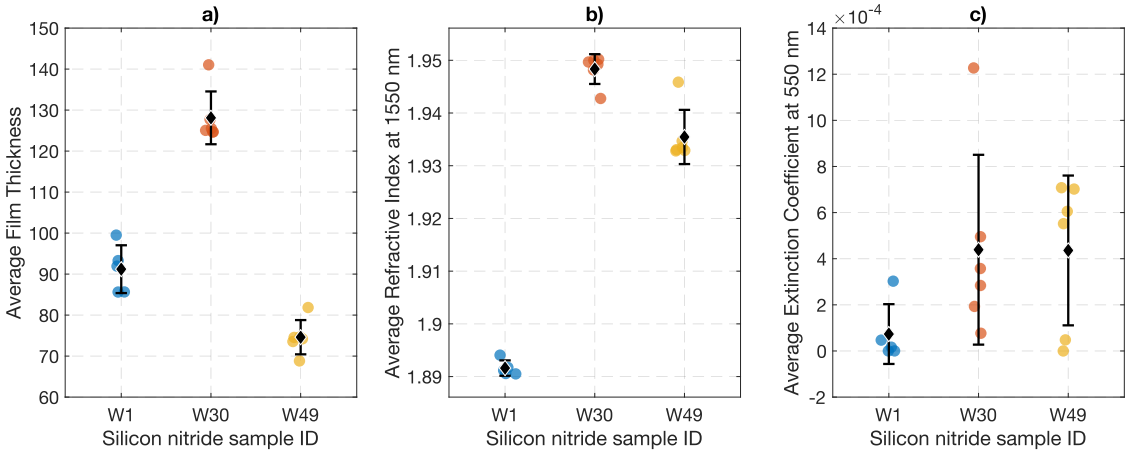

Figure 4.9: Repeated PECVD recipes for estimating the reproducibility of the resulting silicon nitride film properties. The mean value and standard deviation error bars are shown (in black) and W1 denotes the default PECVD recipe. a) Average SiN film thickness across the 4"-wafer. b) Average refractive index across the 4"-wafer at 1550 nm. c) Average extinction coefficient across the 4"-wafer at 550 nm.

To summarise, the accuracy of measurement results and reproducibility of the silicon nitride films formed by the PECVD recipes are important for making good predictions. The reproducibility of SiN films and measurement data is best in terms of refractive index, followed by film thickness, while the obtained extinction coefficient is less reliable. Such deviations can be responsible for discrepancies between targeted and obtained SiN properties of the predicted PECVD recipes.

5
Conclusion

In this thesis, a Design of Experiments (DOE) for investigating process parameters of Plasma Enhanced Chemical Vapour Deposition (PECVD) was created, silicon nitride layers deposited, and measurements regarding the silicon nitride film properties performed. The goal of this thesis was to obtain an overview of how the chosen PECVD process parameters influence the deposited SiN films, how theses factor settings affect each other, and to determine the optimal combination of PECVD factor settings to achieve a silicon nitride layer suitable for integrated photonics.
For this, the optimal design of experiment approach was followed and the statistical software JMP used, to arrive at an experimental design with a suitable number of runs, given the time-constraints. Silicon nitride films with an intended thickness of approximately 100 nm were deposited according to the DoE using PECVD. Measurements of these fabricated SiN films were performed using spectrometric ellipsometry, in order to obtain the refractive index, the extinction coefficient, and the thickness uniformity. By means of this measured data and the respective PECVD factor settings, the prediction profiler in JMP was used to predict PECVD factor setting combinations, that should result in the desired responses of the SiN film. Specifically, a refractive index $n = 2.0$, a minimised extinction coefficient $k < 1 \times 10^{-3}$, and good thickness uniformity (i.e. minimised thickness deviations).
Correlations between the PECVD factors and silicon nitride properties were found, as well as significant interaction effects between the six PECVD factors investigated. The refractive index was found to be significantly affected by all PECVD process parameters with the exception of pressure. The most important factor being the gas flow rate of ammonia, which should be low, if higher refractive indices are to be achieved. The chosen frequency mode and silane gas flow rate can make this relationship even more pronounced. For the extinction coefficient, the gas flow rates of ammonia and nitrogen, as well as the frequency mode seem to matter the most. In addition, a positive correlation was observed between the refractive index and the extinction coefficient, whereby a higher refractive index at 1550 nm tends to be accompanied by an increased extinction coefficient at 550 nm wavelength, indicating increased absorption. As for the thickness uniformity, the choice of frequency mode is essential, with the high frequency mode being most favourable in this regard. The collected data also shows that many relevant two-factor interactions are present in the PECVD deposition process, affecting the relationship between factor settings and desired outcomes.
Regarding the prediction of optimal PECVD factor settings, advances in comparison to the default low frequency PECVD recipe were made. Most predicted recipes performed well or even very well, when considering the whole set of recipes tested.

While improvements in each of the target responses (refractive index, extinction coefficient, and thickness uniformity) were shown, it seems that the target value can not be reached for all three responses simultaneously. However, if the focus of interest lies on the Si/N ratio instead of on the refractive index, simultaneous optimisation can be achieved. In this case, a PECVD recipe was predicted that outperforms the default PECVD and the default LPCVD recipes.
Nevertheless, some lack of clarity remains concerning the prediction of multiple different apparently optimal recipes. In order to determine, why multiple optimal recipes are predicted, what the reasons for this are, and how to unerringly predict the best PECVD factor setting combinations, more predictions need to be systematically performed and these recipes tested. Furthermore, to truly minimise the extinction coefficient a different measurement method has to be used, which can differentiate the performance of the PECVD recipes in this regard for values below the ellipsometer's detection limit. Alternatively, investigating the propagation losses directly, since the losses of devices fabricated using the presented PECVD recipes are the ultimate performance indicator, would be of interest. In this regard, the fabrication of ring resonators is planned in future work, whereby the best PECVD recipes for silicon nitride deposition for the waveguide core are to be tested. Further research on the reproducibility of the deposited SiN films and corresponding measurements, would be beneficial as well for more accurate predictions and confidence in observed trends. Additionally, it would be useful to investigate the performance of the identified promising PECVD recipes when fabricating thicker silicon nitride films. Especially, in the context of ensuring that no detrimental stress issues hinder the fabrication of devices in future.
Overall, the idea of using optimal design of experiment to optimise fabrication related processes for integrated photonics, within a reasonable economic cost framework, is certainly of interest. This approach shows notable potential and with increased experience and insight regarding the statistical tools as well as the relevant fabrication and measurement methods, it could definitely be worth exploring for other fabrication steps affecting waveguide losses, such as etching steps and resulting waveguide sidewall roughness.

Bibliography

[1] M.A. Butt, B. Janaszek and R. Piramidowicz. "Lighting the Way Forward: The Bright Future of Photonic Integrated Circuits". In: *Sensors International* 6 (2025). ISSN: 26663511. DOI: 10.1016/j.sintl.2025.100326.

[2] Chong Zhang et al. "Integrated Photonics beyond Communications". In: *Applied Physics Letters* 123.23 (4th Dec. 2023). ISSN: 0003-6951. DOI: 10.1063/5.0184677.

[3] Roel Baets et al. "Silicon Photonics: Silicon Nitride versus Silicon-on-Insulator". In: *2016 Optical Fiber Communications Conference and Exhibition (OFC)*. 2016 Optical Fiber Communications Conference and Exhibition (OFC). Mar. 2016, pp. 1–3.

[4] Zhichao Ye. "Ultralow-Loss Silicon Nitride Waveguides for Nonlinear Optics". Chalmers University of Technology, 2021. ISBN: 9789179054588. URL: https://research.chalmers.se/en/publication/522499.

[5] Kirill A. Buzaverov et al. "Silicon Nitride Integrated Photonics from Visible to Mid-Infrared Spectra". In: *Laser & Photonics Reviews* 18.12 (2024). ISSN: 1863-8899. DOI: 10.1002/lpor.202400508.

[6] Brahim Ahammou et al. "Mechanical and Optical Properties of Amorphous Silicon Nitride-Based Films Prepared by Electron Cyclotron Resonance Plasma-Enhanced Chemical Vapor Deposition". In: *Journal of Vacuum Science & Technology A* 41.5 (23rd Aug. 2023). ISSN: 0734-2101. DOI: 10.1116/6.0002896.

[7] Chao Xiang, Warren Jin and John E. Bowers. "Silicon Nitride Passive and Active Photonic Integrated Circuits: Trends and Prospects". In: *Photonics Research* 10.6 (1st June 2022), A82–A96. ISSN: 2327-9125. DOI: 10.1364/PRJ.452936.

[8] Roel Baets and Abdul Rahim. "Heterogeneous Integration in Silicon Photonics: Opportunities and Challenges: Opinion". In: *Optical Materials Express* 13.12 (1st Dec. 2023), pp. 3439–3444. ISSN: 2159-3930. DOI: 10.1364/OME.509531.

[9] Chris Yang and John Pham. "Characteristic Study of Silicon Nitride Films Deposited by LPCVD and PECVD". In: *Silicon* 10.6 (Nov. 2018), pp. 2561–2567. ISSN: 1876-990X, 1876-9918. DOI: 10.1007/s12633-018-9791-6.

[10] Zhaoyi Li et al. "Process Development of Low-Loss LPCVD Silicon Nitride Waveguides on 8-Inch Wafer". In: *Applied Sciences* 13.6 (6 Jan. 2023). ISSN: 2076-3417. DOI: 10.3390/app13063660.

[11] Linghua Wang et al. “Nonlinear Silicon Nitride Waveguides Based on a PECVD Deposition Platform”. In: *Optics Express* 26.8 (16th Apr. 2018), pp. 9645–9654. ISSN: 1094-4087. DOI: 10.1364/OE.26.009645.

[12] S. M. Sze and M. K. Lee. *Semiconductor Devices, Physics and Technology*. 3rd ed. Hoboken, N.J: Wiley, 2012. 578 pp. ISBN: 978-0-470-53794-7.

[13] Debapam Bose et al. “Anneal-Free Ultra-Low Loss Silicon Nitride Integrated Photonics”. In: *Light: Science & Applications* 13.1 (8th July 2024). ISSN: 2047-7538. DOI: 10.1038/s41377-024-01503-4.

[14] Shuangyou Zhang et al. “Low-Temperature Sputtered Ultralow-Loss Silicon Nitride for Hybrid Photonic Integration”. In: *Laser & Photonics Reviews* 18.4 (2024). ISSN: 1863-8899. DOI: 10.1002/lpor.202300642.

[15] Thalía Domínguez Bucio. “NH3-free PECVD Silicon Nitride for Photonic Applications”. PhD thesis. Southampton, UK: University of Southampton, 18th June 2018. URL: https://eprints.soton.ac.uk/422874/1/Final_thesis.pdf.

[16] Leonid Yu. Beliaev et al. “Optical, Structural and Composition Properties of Silicon Nitride Films Deposited by Reactive Radio-Frequency Sputtering, Low Pressure and Plasma-Enhanced Chemical Vapor Deposition”. In: *Thin Solid Films* 763 (1st Dec. 2022). ISSN: 0040-6090. DOI: 10.1016/j.tsf.2022.139568.

[17] Yujin Cao et al. “Study on Effect of Process and Structure Parameters on SiNxHy Growth by In-Line PECVD”. In: *Solar Energy* 198 (1st Mar. 2020), pp. 469–478. ISSN: 0038-092X. DOI: 10.1016/j.solener.2020.01.054.

[18] Jicheng Zhou et al. “Multi-Field Simulation and Optimization of SiNx:H Thin-Film Deposition by Large-Size Tubular LF-PECVD”. In: *Solar Energy* 228 (1st Nov. 2021), pp. 575–585. ISSN: 0038-092X. DOI: 10.1016/j.solener.2021.09.075.

[19] Jiju Antony. *Design of Experiments for Engineers and Scientists*. Elsevier, 2014. ISBN: 978-0-08-099417-8. DOI: 10.1016/C2012-0-03558-2.

[20] Rong Tu et al. “High-Speed Deposition of Silicon Nitride Thick Films via Halide Laser Chemical Vapor Deposition”. In: *Journal of the European Ceramic Society* 43.12 (1st Sept. 2023), pp. 5214–5222. ISSN: 0955-2219. DOI: 10.1016/j.jeurceramsoc.2023.04.035.

[21] Dmitrii Belogolovskii et al. “Silicon-Rich Nitride Refractive Index as a Degree of Freedom to Maximize Nonlinear Wave Mixing in Nanowaveguides”. In: *Advanced Photonics Research* 5.10 (2024). ISSN: 2699-9293. DOI: 10.1002/adpr.202400017.

[22] Clifford R. Pollock and Michal Lipson. *Integrated Photonics*. Boston, MA: Springer US, 2003. ISBN: 978-1-4419-5398-8 978-1-4757-5522-0. DOI: 10.1007/978-1-4757-5522-0.

[23] V Lucarini et al. *Kramers-Kronig Relations in Optical Materials Research*. Vol. 110. Springer Series in Optical Sciences. Berlin/Heidelberg: Springer-Verlag, 2005. ISBN: 978-3-540-23673-3. DOI: 10.1007/b138913.

[24] Mikhail N. Polyanskiy. “Refractiveindex.Info Database of Optical Constants”. In: *Scientific Data* 11.1 (18th Jan. 2024). ISSN: 2052-4463. DOI: 10.1038/s41597-023-02898-2.

[25] Thomas Bonnal et al. “How to Determine the Complex Refractive Index from Infrared Reflectance Spectroscopy?” In: *SN Applied Sciences* 2.12 (Dec. 2020). ISSN: 2523-3963, 2523-3971. DOI: 10.1007/s42452-020-03869-7.

[26] *Ellipsometry Tutorial*. J.A. Woollam. URL: https://www.jawoollam.com/resources/ellipsometry-tutorial (visited on 10/07/2025).

[27] Sahar Jafari et al. “Effect of High Temperature Firing on the Bond Configuration and Composition of A-SiN:H Passivation Layer Deposited by PECVD”. In: EU PVSEC. Amsterdam, 2017. URL: https://www.researchgate.net/publication/320300233_Effect_of_high_temperature_firing_on_the_bond_configuration_and_composition_of_a-SiNH_passivation_layer_deposited_by_PECVD.

[28] Zhichao Ye et al. “Low-Loss High-Q Silicon-Rich Silicon Nitride Microresonators for Kerr Nonlinear Optics”. In: *Optics Letters* 44.13 (1st July 2019), pp. 3326–3329. ISSN: 1539-4794. DOI: 10.1364/OL.44.003326.

[29] “Deposition of Thin Films: PECVD Process”. In: *Silicon Based Thin Film Solar Cells*. Ed. by Roberto Murri. BENTHAM SCIENCE PUBLISHERS, 18th Mar. 2013, pp. 29–57. ISBN: 978-1-60805-518-0. DOI: 10.2174/978160805518011301006.

[30] Lian-Qiao Yang et al. “Global Optimization of Process Parameters for Low-Temperature SiNx Based on Orthogonal Experiments”. In: *Advances in Manufacturing* 11.2 (June 2023), pp. 181–190. ISSN: 2095-3127, 2195-3597. DOI: 10.1007/s40436-022-00423-z.

[31] M. A. Lieberman and Allan J. Lichtenberg. *Principles of Plasma Discharges and Materials Processing*. 2nd ed. Hoboken, N.J: Wiley-Interscience, 2005. 757 pp. ISBN: 978-0-471-72001-0.

[32] I. Guler. “Optical and Structural Characterization of Silicon Nitride Thin Films Deposited by PECVD”. In: *Materials Science and Engineering: B* 246 (1st July 2019), pp. 21–26. ISSN: 0921-5107. DOI: 10.1016/j.mseb.2019.05.024.

[33] Xavier X. Chia et al. “Optical Characterization of Deuterated Silicon-Rich Nitride Waveguides”. In: *Scientific Reports* 12.1 (26th July 2022). ISSN: 2045-2322. DOI: 10.1038/s41598-022-16889-7.

[34] Margarita Lapteva et al. “Development of PECVD SiN Thin Films for Integrated Photonic Applications on 300 Mm Wafers”. In: *The 25th European Conference on Integrated Optics*. Ed. by Jeremy Witzens et al. Cham: Springer Nature Switzerland, 2024, pp. 511–515. ISBN: 978-3-031-63378-2. DOI: 10.1007/978-3-031-63378-2_83.

[35] Sungwook Jung, Deayoung Gong and Junsin Yi. “The Effects of the Band Gap and Defects in Silicon Nitride on the Carrier Lifetime and the Transmittance in C-Si Solar Cells”. In: *Solar Energy Materials and Solar Cells* 95.2 (Feb. 2011), pp. 546–550. ISSN: 0927-0248. DOI: 10.1016/j.solmat.2010.09.014.

[36] Reinoud F. Wolffenbuttel et al. “Optical properties of nitride-rich SiNx and its use in CMOS-compatible near-UV Bragg filter fabrication”. In: *Optical Materials: X* 24 (1st Dec. 2024). ISSN: 2590-1478. DOI: 10.1016/j.omx.2024.100348.

[37] Seiya Yoshinaga et al. “The Optical Properties of Silicon-Rich Silicon Nitride Prepared by Plasma-Enhanced Chemical Vapor Deposition”. In: *Materials Science in Semiconductor Processing* 90 (1st Feb. 2019), pp. 54–58. ISSN: 1369-8001. DOI: 10.1016/j.mssp.2018.09.029.

[38] Peter Goos and Bradley Jones. *Optimal Design of Experiments: A Case Study Approach*. 1st ed. Wiley, July 2011. ISBN: 978-0-470-74461-1 978-1-119-97401-7. DOI: 10.1002/9781119974017.

[39] Byran Smucker, Martin Krzywinski and Naomi Altman. “Optimal Experimental Design”. In: *Nature Methods* 15.8 (Aug. 2018), pp. 559–560. ISSN: 1548-7091, 1548-7105. DOI: 10.1038/s41592-018-0083-2.

[40] *JMP 18.2 Help*. JMP Statistical Discovery LLC. 3rd Mar. 2025. URL: https://www.jmp.com/support/help/en/18.2/index.shtml#page/jmp/effect-tests.shtml (visited on 03/08/2025).

[41] Robert W. Collins. “Measurement Technique of Ellipsometry”. In: *Spectroscopic Ellipsometry for Photovoltaics*. Ed. by Hiroyuki Fujiwara and Robert W. Collins. Vol. 212. Cham: Springer International Publishing, 2018, pp. 19–58. ISBN: 978-3-319-75375-1 978-3-319-75377-5. DOI: 10.1007/978-3-319-75377-5_2.

[42] Josef Humlíček. “1 - Polarized Light and Ellipsometry”. In: *Handbook of Ellipsometry*. Ed. by Harland G. Tompkins and Eugene A. Irene. Norwich, NY: William Andrew Publishing, 1st Jan. 2005, pp. 3–91. ISBN: 978-0-8155-1499-2. DOI: 10.1016/B978-081551499-2.50003-4.

[43] Gerald E. Jellison. “3 - Data Analysis for Spectroscopic Ellipsometry”. In: *Handbook of Ellipsometry*. Ed. by Harland G. Tompkins and Eugene A. Irene. Norwich, NY: William Andrew Publishing, 1st Jan. 2005, pp. 237–296. ISBN: 978-0-8155-1499-2. DOI: 10.1016/B978-081551499-2.50005-8.

[44] Fred A. Stevie and Carrie L. Donley. “Introduction to X-Ray Photoelectron Spectroscopy”. In: *Journal of Vacuum Science & Technology A: Vacuum, Surfaces, and Films* 38.6 (1st Dec. 2020). ISSN: 0734-2101, 1520-8559. DOI: 10.1116/6.0000412.

[45] Paul Van der Heide. *X-Ray Photoelectron Spectroscopy: An Introduction to Principles and Practices*. Hoboken, N.J: Wiley, 2012. 241 pp. ISBN: 978-1-118-06253-1.

[46] Nenad Stojilovic. “Why Can’t We See Hydrogen in X-ray Photoelectron Spectroscopy?” In: *Journal of Chemical Education* 89.10 (11th Sept. 2012), pp. 1331–1332. ISSN: 0021-9584, 1938-1328. DOI: 10.1021/ed300057j.

[47] G. E. Jellison and F. A. Modine. “Parameterization of the Optical Functions of Amorphous Materials in the Interband Region”. In: *Applied Physics Letters* 69.3 (15th July 1996), pp. 371–373. ISSN: 0003-6951, 1077-3118. DOI: 10.1063/1.118064.

[48] *Ellipsometry FAQ*. J.A. Woollam. URL: https://www.jawoollam.com/resources/ellipsometry-faq (visited on 10/07/2025).

[49] Mateus Corato-Zanarella et al. “Absorption and Scattering Limits of Silicon Nitride Integrated Photonics in the Visible Spectrum”. In: *Optics Express* 32.4 (12th Feb. 2024). ISSN: 1094-4087. DOI: 10.1364/OE.505892.

[50] Clemens Krückel. “Integrated Nonlinear Optics in Silicon Nitride Waveguides”. Chalmers University of Technology, 2017. ISBN: 9789175975542. URL: https://research.chalmers.se/en/publication/248868.

[51] Matteo Barcellona et al. “Differences in HF Wet Etching Resistance of PECVD SiNx:H Thin Films”. In: *Materials Chemistry and Physics* 306 (15th Sept. 2023). ISSN: 0254-0584. DOI: 10.1016/j.matchemphys.2023.128023.

[52] Jiseok Lee, Jiwon Jang and Sang Jeen Hong. “Understanding the Chamber Wall-Deposited Thin Film of Plasma Deposition Equipment for the Efficiency of In Situ Dry-Cleaning”. In: *Coatings* 15.5 (8th May 2025). ISSN: 2079-6412. DOI: 10.3390/coatings15050563.

A

Appendix

Results from effect tests, PECVD recipes, and measurement data that are not shown in the main body of the thesis are listed here in the following tables.

Table A.1: Significant effects and their corresponding p-values obtained during effect tests. The investigated response is the refractive index of the 38 silicon nitride samples fabricated according to the DoE.

Source	Effect Type	p-value
Power	main effect	0.0009
Frequency Mode	main effect	< 0.0001
Silane	main effect	< 0.0001
Ammonia	main effect	< 0.0001
Nitrogen	main effect	0.0002
Pressure * Silane	2-factor interaction effect	0.0209
Power * Frequency Mode	2-factor interaction effect	0.0044
Power * Ammonia	2-factor interaction effect	0.0055
Frequency Mode * Silane	2-factor interaction effect	0.0173
Frequency Mode * Ammonia	2-factor interaction effect	< 0.0001
Frequency Mode * Nitrogen	2-factor interaction effect	0.0191
Silane * Ammonia	2-factor interaction effect	0.0007
Silane * Nitrogen	2-factor interaction effect	< 0.0001
Ammonia * Nitrogen	2-factor interaction effect	0.0153
Ammonia * Ammonia	quadratic effect	< 0.0001

Table A.2: Significant effects and their corresponding p-values obtained during effect tests. The investigated response is the normalised film thickness standard deviation across the wafers of the 38 silicon nitride samples fabricated according to the DoE.

Source	Effect Type	p-value
Frequency Mode	main effect	0.0075
Pressure * Frequency Mode	2-factor interaction effect	0.0042
Pressure * Silane	2-factor interaction effect	0.0198
Pressure * Nitrogen	2-factor interaction effect	0.0374
Power * Silane	2-factor interaction effect	0.0273
Power * Ammonia	2-factor interaction effect	0.0015
Silane * Ammonia	2-factor interaction effect	0.0481

Table A.3: Significant effects and their corresponding p-values obtained during effect tests. The investigated response is the extinction coefficient of the 38 silicon nitride samples fabricated according to the DoE.

Source	Effect Type	p-value
Frequency Mode	main effect	0.0007
Ammonia	main effect	< 0.0001
Nitrogen	main effect	0.0033
Pressure * Power	2-factor interaction effect	0.0318
Frequency Mode * Ammonia	2-factor interaction effect	< 0.0001
Frequency Mode * Nitrogen	2-factor interaction effect	0.0158
Ammonia * Nitrogen	2-factor interaction effect	0.0043

Table A.4: Optimal Design of Experiment containing the 38 PECVD recipes. LF, MF, and HF denote low frequency, mixed frequency, and high frequency mode, respectively.

Recipe ID	Pressure (mTorr)	Power (W)	Frequency Mode	5 % SiH4 (sccm)	NH3 (sccm)	N2 (sccm)
15	1900	100	LF	295	0	100
16	1900	100	MF	490	22.5	850
17	650	100	HF	490	45	100
18	1900	60	MF	100	0	850
19	1275	20	MF	100	22.5	1600
20	1900	60	LF	490	45	100
21	650	100	MF	100	45	100
22	1900	20	MF	295	22.5	100
23	650	20	MF	295	5	850
24	650	100	LF	100	45	100
25	650	20	HF	490	0	1600
26	650	100	HF	100	45	1600
27	650	100	LF	490	7.5	850
28	650	20	LF	295	45	1600
29	1275	60	HF	295	22.5	850
30	650	60	LF	100	0	1600
31	1275	20	MF	490	45	850
32	1275	20	LF	100	2.5	100
33	1900	20	HF	100	0	1600
34	1275	60	LF	295	22.5	850
35	1275	100	MF	295	0	1600
36	1900	100	HF	100	45	100
37	1900	100	LF	100	22.5	1600
38	1900	20	HF	490	45	1600
39	1275	60	HF	295	22.5	850
40	1900	20	LF	100	45	850
41	650	100	HF	100	0	100
42	1275	60	HF	295	22.5	850
43	650	20	HF	100	45	100
44	1900	60	MF	295	45	1600
45	650	60	MF	490	22.5	1600
46	1900	100	HF	490	0	1600
47	1900	20	HF	490	0	100
48	1275	60	MF	490	0	100
49	650	20	LF	490	22.5	100
50	1275	100	LF	490	45	1600
51	1900	20	LF	490	10	1600
52	1275	60	MF	100	45	100

DEPARTMENT OF MICROTECHNOLOGY AND NANOSCIENCE
CHALMERS UNIVERSITY OF TECHNOLOGY
Gothenburg, Sweden
www.chalmers.se

CHALMERS
UNIVERSITY OF TECHNOLOGY